Snow mechanical properties variability at the slope scale, implication for snow mechanical modeling

Francis Meloche[1,3], Francis Gauthier[1,3], and Alexandre Langlois[2,3]

[1]Laboratoire de géomorphologie et de gestion des risques en montagnes (LGGRM), Département de Biologie, Chimie et Géographie, Université du Québec à Rimouski, Canada.
[2]Groupe de Recherche Interdisciplinaire sur les Milieux Polaires (GRIMP), Département de géomatique appliquée, Université de Sherbrooke, Canada.
[3]Center for Nordic studies, Université Laval, Québec, Canada.

Correspondence: Francis Meloche (francis.meloche@uqar.ca)

Abstract. Snow avalanches represent a natural hazard for infrastructures and backcountry recreationists. Risk assessment of avalanche hazard is difficult due to the sparse nature of available observations informing on snowpack mechanical and geophysical properties and overall stability. The spatial variability of these properties also adds complexity to the decision-making and route finding in avalanche terrain for mountain users. Snow cover models can simulate snow mechanical properties with good accuracy at fairly good spatial resolution (around 100 m). However, monitoring small-scale variability at the slope scale (5-50 m) remains critical, since slope stability and the possible size of an avalanche are governed by such a scale. To better understand and estimate the spatial variability at the slope scale, this work explores existing links between snow mechanical properties and microtopographic indicators. First, we compared the covariance models of snow mechanical properties and stability metrics between surveys. Then, we estimated snow mechanical properties, including point snow stability, using GAM spatial models (Generalized Additives Models) with microtopographic indicators as covariates. Snow mechanical properties such as snow density, elastic modulus, shear modulus and snow microstructural strength were estimated from a high-resolution snow penetrometer (SMP) at multiple locations over several studied slopes, in Rogers Pass, British-Columbia, and Mt Albert, Québec. Point snow stability such as the skier crack length, critical propagation crack length and a skier stability index were derived using the snow mechanical properties from SMP measurements. Microtopographic indicators such as the topographic position index (TPI), vegetation height and proximity, Up-wind slope index (wind exposed/sheltered area) and potential radiation index were derived from Unmanned Aerial Vehicles (UAV) surveys with sub-meter resolution. We computed the variogram and fractal dimension of snow mechanical properties. The comparison showed some similarities in the correlation distances and fractal dimensions between the slab thickness and the slab snow density and also between the weak layer microstructural strength and the stability metrics. The use of covariates in GAM models suggested that microtopographic indicators can be used to predict the snow mechanical properties, and with less precision, stability metrics. The snow stability maps that were generated represent good teaching material in avalanche skill training and awareness courses. The difference in spatial pattern between the slab and the weak layer should be considered in snow mechanical modeling.

1 Introduction

Snow avalanches represent a natural hazard for infrastructures and backcountry recreationists across mountainous areas all
across the world (Stethem et al., 2003; Techel et al., 2016). Snow avalanches can be divided into different types of avalanches:
wet, dry, non-cohesive or slab avalanches. However, dry-snow slab avalanches are the most difficult to predict and the ones
causing the most fatalities (Techel et al., 2016). It requires a shear crack usually initiated by a person or new stresses from
snowfall or warming in a weak porous layer underneath a cohesive snow slab. Then, the crack must be at a critical length in
order to self-propagate across the slope for a slab avalanche to occur. Practitioners and forecasters estimate the probability
and size of an avalanche from punctual information on weak layers and slab properties across different scales. However, the
sparse and punctual nature of available observations on snowpack properties makes the forecasting of dry snow slab avalanches
difficult (Hägeli and McClung, 2004). The snow spatial variability at different scales also adds complexity to this challenging
task by adding uncertainty on whether the properties measured in the field are representatives of the slab and weak layer system
(Schweizer et al., 2008a).

The spatial variability of snow properties is well documented in climate studies (e.g. Harper and Bradford, 2003), glacier
dynamics (e.g. Pulwicki et al., 2018), snow hydrology (e.g. Deems et al., 2006), mountain meteorology (Mott et al., 2011),
permafrost (e.g. Wirz et al., 2011) and snow avalanche (e.g. Schweizer et al., 2008a). Several studies have looked at the spatial
distribution of snow depth and its water equivalent to feed hydrological models (e.g. Deems et al., 2006; Grünewald et al.,
2010; Schirmer et al., 2011; Winstral et al., 2002). Some authors went further to estimate and analyze the spatial pattern of
snow depth (Deems et al., 2006; Mott et al., 2011; Schirmer and Lehning, 2011; Trujillo et al., 2007). They analyzed the scaling
properties and the fractal dimension of the snow depth, which can be estimated with the slope of a log-log variogram or with
the periodogram of the spatial signal. The idea behind the scaling properties and fractal dimension is that many scales can
define a spatial pattern instead of one scale like the correlation length in a variogram. Fractal dimension can also characterize
the roughness or smoothness of a spatial pattern over multiple scales. These authors compared the fractal dimension of snow
depth with the fractal dimension of topographic indicators and vegetation. However, no study has studied the fractal dimension
of snow mechanical properties. Most of these studies are mainly based on LiDAR or manual snow probe surveys to estimate
the snow depth. However, snow depth is not a good indicator of the conditions required for snow avalanches to occur.

There are better indicators, such as snow stability tests, to estimate the conditions for snow avalanches. These tests are
widely used in the avalanche industry to assess snow stability and, ultimately, snow avalanche hazard. The result of these
tests represents a qualitative evaluation of the mechanical interaction between the cohesive slab and the weak layer. Some
studies investigate the variability of several snow stability tests on an avalanche-prone slope (Kronholm and Schweizer, 2003;
Birkeland, 2001; Campbell and Jamieson, 2007). These results demonstrate a variation in the test results and spatial patterns
with variograms and correlation distances around 5-20 m. However, these snow stability tests do not provide information on
the snow mechanical properties of the slab and the weak layer. Snow stability tests are also time-consuming, causing the spatial
sampling density and extent to be relatively small for statistical analysis, around 20 m and below 30 measurements. The ~~high
resolution~~ high-resolution snow penetrometer, Snowmicropen (SMP), is used to characterize the mechanical and structural

properties of the snow, ~~of the snow,~~ such as the thickness of the slab and the weak layer, the density, the elastic modulus, and the microstructural strength of the weak layer (Proksch et al., 2015; Löwe and van Herwijnen, 2012; Johnson and Schneebeli, 1999). Several authors characterized stability based on snow mechanical properties of the slab and the weak layer (Föhn, 1987;

60 Gaume and Reuter, 2017; Reuter et al., 2015b; Monti et al., 2016; Schweizer and Reuter, 2015; Reuter and Schweizer, 2018; Rosendahl and Weißgraeber, 2020). Gaume and Reuter (2017) proposed a stability index that represents both failure initiation and propagation propensity with an analytical method that can be easily applied to SMP profiles.

The SMP was used in snow spatial studies because it can rapidly and accurately measure the mechanical properties of the snow relevant to snow stability on a slope prone to avalanche (Bellaire and Schweizer, 2011; Feick et al., 2007; Kronholm

65 and Schweizer, 2003; Landry et al., 2004; Lutz et al., 2007; Lutz and Birkeland, 2011). These studies report spatial patterns of weak layer properties with a correlation distance ranging from 0.5 to 20 m. However, the sampling density and the spatial extent of the survey were around 20 to 50 m for the spatial extent and between 20 to 50 SMP measurements depending on the studies. Reuter et al. (2016) also used stability metrics based on snow mechanical properties derived from the SMP to show spatial patterns of snow stability with a larger sampling density and extent compared to the other studies. The correlation

70 distance obtained from this study was still in the same range as the others with some exceptions between 40 and 60 m. The spatial patterns of snow instability differed between the surveys, and these results were attributed to the different meteorological processes interacting with the terrain and the snow cover (e.g. Schweizer et al., 2008a; Reuter et al., 2016).

From these results, several studies simulated artificial spatial patterns of the weak layer in mechanical models to explain the effect of the spatial variability of the weak layer on the slope stability, given the likelihood of an avalanche (Gaume et al.,

75 2014, 2013; Kronholm and Birkeland, 2005; Fyffe and Zaiser, 2004). Gaume et al. (2015) used the same method to estimate the propensity for tensile failure in the slab and the relationship with the size of the avalanche release. These studies were based on the assumption that the spatial patterns of the weak layer ranged from 0.5 to 10 m, with the other parameters being constant for simplicity. Bellaire and Schweizer (2011) suggested that the spatial patterns of the weak layer and the slab could have different correlation distances for the same survey. However, the spatial extent of the snow sampling was relatively small, only

80 twice as the measured correlation length, and could affect the estimation of the correlation length (e.g. Dale and Fortin, 2014; Skøien and Blöschl, 2006). The slab and the weak layer could have a different spatial pattern, resulting in some cases with a slab variation smoother than the weak layer or the opposite. This matter should be further explored with a spatial sampling extent greater than 20 m in order to improve the implementation of snow variability in mechanical models.

Spatial patterns of snow properties can also be explained and estimated by statistical models with exploratory spatial vari-

85 ables. In the past, environmental variables were mapped using a linear regression model and kriging with external drift. Several studies used kriging to map point snow stability, such as snow stability test results, SMP-derived mechanical properties, and stability metrics (Birkeland, 2001; Mullen and Birkeland, 2008; Reuter et al., 2015a; Schweizer and Kronholm, 2007). These studies showed that point snow stability can be partially explained using topographic indicators such as aspect, altitude, and slope angle on the regional / massif scale. These topographic indicators can express the complex interactions between the

90 meteorological process and the terrain, such as wind deposition from lee / windward slopes and solar radiation on the snow surface between different slopes (Reuter et al., 2016). However, spatially autocorrelated residuals remained from these statis-

tical models using topographic indicators. This remaining spatial variability could be explained and estimated by other spatial phenomena on a smaller scale. At the slope scale, other authors explained and estimated spatial variability of snow depth where slope, aspect, and altitude remained mostly stable (e.g. Deems et al., 2006; Grünewald et al., 2010; Pulwicki et al., 2018; Revuelto et al., 2020; Meloche et al., 2022; Trujillo et al., 2007; Winstral et al., 2002). They used microtopographic indicators such as the shape of the slope (topographic position index TPI), vegetation index and microclimate indexes such as wind exposure (Winstral index) or the potential of solar radiation. Guy and Birkeland (2013) has shown the potential to use microtopography to spatially estimate potential trigger zones, but the characterization of their potential trigger was only with the presence of depth hoar layers. However, the presence of depth hoar crystals to characterize snow stability is insufficient and requires more information on snow mechanical properties for the slab and the weak layer. These mechanical properties can be accurately measured with the SMP (Reuter et al., 2019). No studies have linked snow stability and mechanical properties with microtopography indicators in spatial modeling. This could lead to ~~a more accurate~~ an improvement of the potential avalanche size mapping (Veitinger et al., 2016)~~using the variation~~, but integrating variations of the snow mechanical properties as input in snow mechanical modeling. Also, the spatial studies cited above explored linear relations between point snow stability and topographic indicators, but Reuter et al. (2016) suggests that non-linear relationships should be explored. Other statistical models like General Additive Models (GAM's) can represent ~~nonlinear~~ non-linear relationships and should be explored.

The snow mechanical variability can also affect the overall slope stability with the so-called knockdown effect (Fyffe and Zaiser, 2004; Gaume et al., 2014; Kronholm and Schweizer, 2003; Schweizer et al., 2008a), promoting an overall failure of the slope with long-scale spatial variation of snow mechanical properties. Spatial variation in snow can also affect the size of the avalanche release (Gaume et al., 2015), when small-scale variation can promote slab tensile failure and smaller ~~avalanche~~avalanches. It is necessary to spatially explain and estimate the mechanical properties of the snow and the stability of the snow with microtopography indicators at the slope scale. This study is based on the limitations and suggestions of Reuter et al. (2016), who was able to predict the spatial variation of two stability metrics at a larger scale with terrain-based indicators such as slope, aspect and elevation. This work will attempt to predict the spatial variation at a smaller scale using microtopographic indicators with a non-linear regression. As such, the main objectives of this paper are to compare the scaling effect of the snow mechanical properties and the stability metrics for slopes prone to avalanches with different characteristics and spatially estimate the snow spatial variability using microtopography indicators. A supplementary objective will be to compare the parametrization of snow mechanical properties in relation to the slab thickness to our dataset to improve snow mechanical modeling.

2 Data and methods

2.1 Study sites

In order to spatially estimate the spatial variability of snow using microtopography indicators, we choose three study sites according to their specific microtopography and microclimate context. The first study site was located on Mount Albert in Gaspésie National Park, Québec, Canada (Fig. 1b). The winter climate of the region is characterized by extreme changes caused

by 1) low-pressure continental systems that bring heavy snowfall up 100 cm in 48 hours followed by Artic cold air masses with strong northwestern winds, 2) warm and wet air masses coming from the south creating rain-on-snow events (Meloche et al., 2018). The study site is named Arete de Roc (AR) and is located in a subalpine/tundra area heavily affected by wind and snow transport compared to the other sites. This site has a high soil roughness with large boulders and small trees (1 m high). The slope angle is constant (33°) with a convex roll at the top and a concavity at the bottom (Fig. 1). Two other surveys in Mt Albert at Épaule du Mur (EP) is added for our supplementary objective, adding more dense and thicker slabs in our comparison to classic snow mechanical properties parametrization in relation to slab thickness (Bažant et al., 2003; McClung, 2009a). These two surveys were not used for the spatial analysis because their spatial density and extent are insufficient compared to the other surveys.

Two study sites are in Glacier National Park, located in Rogers Pass, British Columbia, Canada (Fig. 1). Our study sites are on Mount Fidelity, which receives heavy snowfall precipitation (Hägeli and McClung, 2003), and a snow cover of around 2-3 m and sometimes up to 4 m. The Mount Fidelity area is classified as a Transitional snow and avalanche climate influenced by warm and wet air masses from the Pacific that bring heavy snowfall and cold air masses from the North, leading to the development of persistent weak layers (Hägeli and McClung, 2003). This study area experiences annually several persistent weak layers consisting of buried surface hoars or facets, relevant for stability assessment purposes. The first study site at Mount Fidelity is located just above the tree line at 2300 m.a.s.l on a shoulder named Round Hill (RH). This site is an alpine area with low soil roughness (Fig. 1). The slope angle is relatively low (near 25°), with longer and smoother convex rolls around 20-30m. The last study site, Jim Bay Corner (JBC), is located below the tree line at 1830 m.a.s.l. It is an open forested area with relatively low soil roughness with small shrubs. The site has 10 m tall trees which created some shaded areas and the slope angle is relatively constant (near 20°) with small convex rolls around 5-10 m (Fig. 1).

2.2 Data collection and sampling strategies

This study presents 4 snow spatial surveys collected during winter 2021-2022 (Fig. 1): 25 February 2022 at the Arête de Roc site (AR22-PP), 27 January 2022 at the Round Hill site (RH22-PP), 19 January 2022 at Jim Bay corner (JBC22-SH), and 24 January 2022 at Jim bay corner (JBC22-PP). A summary of these surveys will be presented first in 3.1. Snow mechanical properties were measured using the high-resolution SMP. To compare the spatial pattern of snow mechanical properties and snow stability, each SMP measurement was made following a sampling scheme following the concept of the scale triplet which is the support, spacing, and extent described by Blöschl and Sivapalan (1995). The support is the diameter of the SMP penetration cone tip which is around 5 mm with a 1 mm vertical resolution. This ensures a proper estimation of the snow mechanical properties because they are linked to their microstructural properties at the mm scale. A minimum spacing of 2 m and a study site extent of around 60 to 100 m were chosen in order for the spacing to be at least half of the estimated correlation length reported by the literature and the extent needs to be two to five times the estimated correlation, which is around 5-20 m reported by several studies (Bellaire and Schweizer, 2011; Lutz et al., 2007; Reuter et al., 2016; Schweizer and Reuter, 2015). This method ensures a proper estimation of the spatial pattern, defined by the spatial variance and the autocorrelation distance (Skøien and Blöschl, 2006; Dale and Fortin, 2014). Our sampling scheme also needs to be adequate for the second objective, which is the spatial
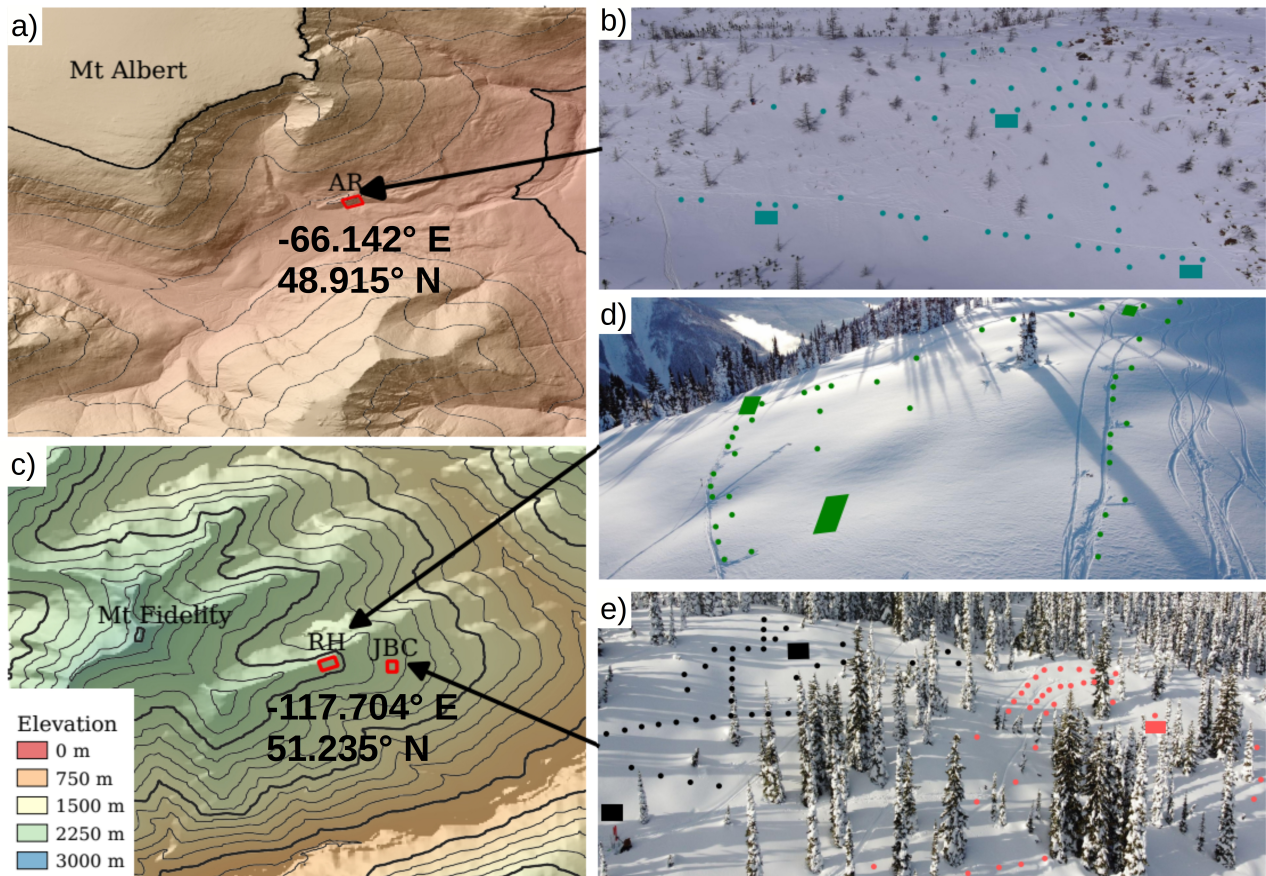
Figure 1. Map of the study area of a) Mount Albert, Québec, Canada, representing the study site b) Arête de Roc with the 25 February 2022 survey in blue (AR). c) Mount Fidelity study area, British Columbia, Canada, with the study sites: d) Round Hill (RH) with the 27 January 2022 survey in green and e) Jim Bay corner (JBC) with the 19 January 2022 survey in red and the 24 January 2022 survey in black. The aerial photography is from the UAV flight of each study site and the snow spatial sampling is represented by circles for the locations of SMP measurements and the squares are the snow profile locations.

estimation of snow mechanical properties and stability metrics using microtopographic indicators. Therefore, the sampling scheme was adjusted for each specific study site in order to obtain a representative distribution of microtopographic indicator values while respecting the scale triplets mentioned above. The sampling was conducted by randomly traversing the study site while adhering to the minimum spacing, and also by characterizing the down and cross-slope for an isotropic sampling. The sampling was stopped when the study site was almost covered with 60 to 80 SMP measurements. The resulting sampling is shown in Figure 1. Random sampling helps to have a good estimation of spatial parameters with limited samples (Kronholm and Birkeland, 2007; Skøien and Blöschl, 2006).

In order to correctly interpret the SMP signal, the weak layer needed to be identified and characterized from a "test" snow profile. Full characterization of the snow stratigraphy was not needed for our analysis, so a shorter version that we called the "test" snow profile was used to optimize the time on the field. Two or three test snow profiles were made per snow spatial survey at least 20 m apart next to SMP measurements (Fig. 1). In each test snow profile, we first performed two compression snow tests to identify the weak layer (Canadian Avalanche Association, 2016). The weak layer was attributed to ~~uppermost compression tests results which was~~ the uppermost compression test results which were consistent in both compression tests. Then, we visually characterized the types and sizes of the snow grains of the weak layer, and finally, a propagation saw test was performed to measure the critical crack length of the weak layer (Gauthier and Jamieson, 2008). We considered every layer above the weak layer to be part of the slab. This assessment enables us to correctly identify the weak layer to the nearest SMP profile and then identify the weak layer in the remaining SMP profiles. Each snow measurement, SMP or snow profile, was georeferenced using a GNSS receiver with centimeter accuracy. In addition to snow measurements, aerial imagery was captured by a quad-rotor UAV with RGB sensor for each study site to characterize the topography in the summer and ~~also in winter at~~ in winter on the same day of the spatial snow survey to characterize the snow surface. Ground / surface models were generated using a *structure from motion (sfm)* photogrammetry algorithm (Westoby et al., 2012) with ground and snow control points to georeference models with centimeter accuracy (< 2 cm in x,y and < 5 cm in z).

2.3 Snow mechanical properties and stability metrics

This section will present the workflow used to process every SMP profile in order to obtain several snow mechanical properties needed for stability assessment. Three stability metrics were then found using these snow mechanical properties. Figure 2 presents the summary of this workflow.

2.3.1 SMP signal processing and snow properties

Each SMP signal was visually interpreted to identify the layers. First, the weak layer was identified on the SMP signal next to the snow profile, with the corresponding depth of the compression test. Then homogeneous layers above the weak layer were classified into slab layers (S_1, S_2,...S_i). This procedure was repeated to the rest of the remaining SMP signal. To obtain the macroscopic mechanical properties of snow for each snow layer, the SMP signal was analyzed using a Poisson shot noise model with a moving window of 2.5 mm. This analysis is used to recover microstructural parameters such as the peak force F, the deflection at rupture δ, and the element length L (Löwe and van Herwijnen, 2012). Then, each structural and macroscopic snow

mechanical property needed to estimate the stability metrics can be retrieved: the slab thickness D, the weak layer thickness D_{wl}, the slab density ρ, the weak layer density ρ_{wl}, the elastic modulus of the slab E and the shear strength of the weak layer τ_p. First, the slab thickness D and the weak layer thickness D_{wl} are extracted directly from the SMP profile. Then, slab density ρ and weak layer density ρ_{wl} are derived using the F and L parameters based on the method proposed by Proksch et al. (2015):

$$\rho = 295.8 + 65.1ln(F) - 43.2ln(F)L + 47.1L, \tag{1}$$

where ρ is in kg m^{-3}, L in mm and F in N. The ~~constant parameters~~ coefficients were obtained by Calonne et al. (2019). The slab density ρ is the mean value of all sub-slab layers above the weak layer and ρ_{wl} is the mean value of the signal inside the weak layer. The effective macroscale elastic modulus of the slab (E) was derived with the new formulation recently adapted by Reuter et al. (2019) originally developed by Johnson and Schneebeli (1999).

$$E = 880\frac{F\delta}{L^3} \cdot \frac{\delta}{L}, \tag{2}$$

The SMP cannot measure specifically the shear strength of the weak layer because of the mixed-mode loading on the weak layer due to the slope angle on the field. Reuter et al. (2015a) previously assumed that the shear strength of the weak layer τ_p is approximately equal to the microstructural strength of the element defined by $\sigma_{micro}^{th} = F/L^2$. We used the same assumptions but used the macroscale strength σ_{macro}^{th} (eq.3), which is the same formulation but scaled with the number of active contacts $\frac{\delta}{L}$ over the 2.5 mm processing moving window of the SMP, following the formulation of Johnson and Schneebeli (1999).

$$\sigma_{macro}^{th} = \frac{F}{L^2} \cdot \frac{\delta}{L} \tag{3}$$

Therefore, we assumed that the shear strength of the weak layer is equivalent to the macro-structural strength of the weak layer $\tau_p \equiv \sigma_{macro}^{th}$.

2.3.2 Stability metrics

The skier propagation index (SPI) proposed by Gaume and Reuter (2017) was used to describe the skier stability. The SPI is the ratio of two lengths: the skier crack length l_{sk} and the critical crack length a_c. The skier crack length defines the length of the crack in the weak layer that will be induced by the weight of a skier staying on top of a slab. The critical crack length is the length of the crack required to begin a dynamic crack propagation. The skier crack length is computed by solving the equation: $\tau + \Delta\tau = \tau_p$, where $\tau = \rho g D sin\psi$ is the shear stress due to the slab weight with g as the gravitational acceleration, and $\Delta\tau$, is the stress due to the skier defined by (Föhn, 1987):

$$\Delta\tau = \frac{2Rcos\alpha sin^2\alpha sin(\alpha + \psi)}{\pi D_e}, \tag{4}$$

where R is the skier load set to 780 N and ψ is the snow surface slope angle derived from UAV imagery, α is the angle between the point at the snow surface under the skier load to the point of maximum induced shear stress at the weak layer, and D_e is

the new multilayered slab thickness, replacing the D only for the skier stress Eq.(4). Slabs are often ~~composed~~ made up of multiple layers with different properties that can affect stress redistribution and potentially damage the weak layer (Habermann et al., 2008; Monti et al., 2016; Weißgraeber and Rosendahl). To account for this process, the method following equations 2,3,4 in Monti et al. (2016), is used to obtain a new equivalent multilayered slab thickness (D_e) based on each layer elastic modulus E that composed the slab. For example, a slab can be composed of many soft layers and one rigid layer with a very high elastic modulus (ex. melt-freeze crust). This slab would have an equivalent thickness D_e compared to D. Then, the roots of the equation are found where $\tau + \Delta\tau = \tau_p$. The roots defined two angles, α_1 and α_2, describing the area of stress from the surface beneath the skier to the weak layer. From these two angles, we found the skier crack length (l_{sk}) with the following equation (Gaume and Reuter, 2017):

$$l_{sk} = D_e \left[\frac{1}{tan\alpha_1} - \frac{1}{tan\alpha_2} \right]. \tag{5}$$

It is important to note here that D_e is only used in the l_{sk} formulation, and the real slab thickness D is still used in the a_c formulation, explained below, and in the spatial analysis and estimation.

The critical crack length is computed using the formulation from Gaume et al. (2017):

$$a_c = \Lambda \left[\frac{-\tau + \sqrt{\tau + 2\sigma(\tau_p - \tau)}}{\sigma} \right], \tag{6}$$

where $\sigma = \rho g D cos\psi$ and Λ is a characteristic length of the system defined by:

$$\Lambda = \sqrt{\frac{E' D D_{wl}}{G_{wl}}}, \tag{7}$$

with $E' = E/(1 - v^2)$, v is the Poisson ratio set to 0.3, D_{wl} is the weak layer thickness and G_{wl} is the shear modulus of the weak layer. However, Richter et al. (2019) proposed to change the formulation of Λ to not use D_{wl} due to the sensitivity of this parameter in snow cover modeling (SNOWPACK), which is also sensitive in the visual interpretation of an SMP profile. They proposed to use a F_{wl} parametrization based on the weak layer density and the optical grain size, replacing the ratio $\frac{D_{wl}}{G_{wl}}$ into the characteristic length $\Lambda = \sqrt{E' D F_{wl}}$. They normalized the optical grain size with a critical grain size (1.25 mm) from Schweizer et al. (2008b). The critical grain size of 1.25 mm comes from statistical analysis, which determines a grain size threshold that classifies stable snow from unstable. We choose to use the same approach, but with the parameters of the SMP L to replace the optical grain size, and we use a critical L_0 of 1.09 mm (Pielmeier and Marshall, 2009), which also classifies a stable and unstable snowpack from the same statistical analysis.

$$F_{wl} = 4.7 \times 10^{-9} \left(\frac{\rho_{wl}}{\rho_{ice}} \cdot \frac{L_{wl}}{L_0} \right)^{-2.1} [\text{mPa}^{-1}] \tag{8}$$

where ρ_{wl} is the weak layer density, L_{wl} is the L parameter from the SMP signal averaged in the weak layer. The values are slightly different from those reported by Richter et al. (2019). Critical crack lengths were also obtained in the field with the propagation saw test (PST) next to the snow profile for each snow sampling survey. We compare the critical crack lengths a_c from the SMP with the critical crack length from the PST tests to validate our approach. It is important to note here that the goal
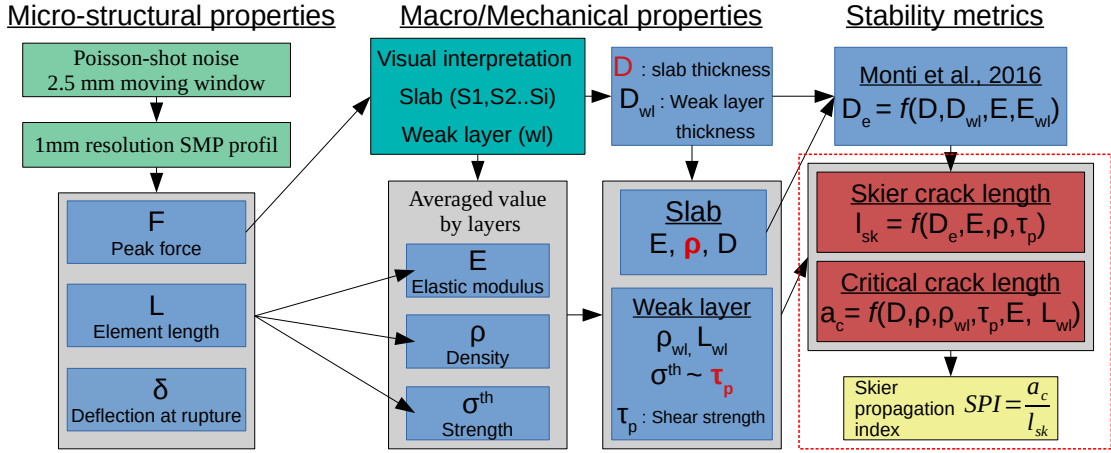
Figure 2. Schematic representation of the workflow used to process the SMP signal to obtain the snow mechanical properties and the stability metrics. The variables and the dashed square in red are the snow mechanical properties and the three stability metrics that will be analyzed and spatially estimated in this work. The parameters of the weak layer are denoted by the subscript X_{wl}.

of the study is not to predict with high accuracy the stability metrics, but to model the spatial variation. The skier propagation index SPI is defined by the critical crack length (a_c) over the skier crack length (l_{sk}) (Gaume and Reuter, 2017):

$$SPI = \frac{a_c}{l_{sk}} \tag{9}$$

A stable snowpack with a skier standing on top will be above 1 and an unstable snowpack below 1.

2.4 Analysis of spatial pattern

The first objective of this paper is to compare the scaling effect on snow mechanical properties and stability metrics for slopes prone to avalanches with different characteristics. We choose three mechanical properties, the slab thickness D, slab density ρ_{slab} and the shear strength of the weak layer τ_p, and also the three stability metrics described above, which are the skier crack length l_{sk}, the critical crack length a_c and the skier propagation index SPI. The spatial pattern of each snow mechanical properties and stability metrics mentioned above were compared between the snow spatial surveys as an exploratory analysis. The omnidirectional sample variogram y was computed following the equation for a variable x (Chilès and Delfiner, 1999).

$$\gamma(h) = \frac{1}{2N} \sum_{i=1}^{N} [(x_i + h) - x_i]^2 \tag{10}$$

with N = number of observations and h = distance between observations. The experimental variogram is defined by three parameters, the nugget or the non-spatial variance, the sill, which is the spatial variance, and the correlation length, which is the distance where the variance stabilized. The sill is difficult to compare between properties because they do not have the same units. However, the correlation length will be compared between snow mechanical properties and stability metrics

because they share the same unit. The correlation length gives an indication of the size of the spatial pattern. ~~Covariance models~~ Four different types of covariance models (Gaussian, Exponential, Spherical, Matern) were fitted to the experimental variogram using ~~the~~ iterative reweighted least squares estimation with function fit.variogram from the *gstat* package in Rstudio (R Core, 2013). The fractal dimension expresses the roughness or complexity of a segment (1-2D), a surface (2-3D), or a volume (3-4D), in a noninteger dimension (Gao and Xia, 1996). From the variogram, we estimate the slope ϕ of the transformed log-log variogram, then follow this equation to get the fractal dimension:

$$d_{fractal} = 3 - (\frac{\phi}{2}) \tag{11}$$

2.5 Spatial modeling

2.5.1 Covariates processing

The second objective of this study is to explore the link between microtopographic indicators and snow mechanical properties and stability metrics to explain and estimate snow spatial variability. The scale of these microtopographic indicators is defined by the size of the moving window used. Different sizes of moving windows were used to allow a multiscale approach in describing the spatial process (e.g. Revuelto et al., 2020; Meloche et al., 2022; Veitinger et al., 2014). The different sizes of the moving window used in this study are based on the literature and will be developed further below. Microtopography indicators are used as exploratory spatial variables and will be referred to as covariates in the spatial model. These covariates were generated from a digital terrain and surface model (DTM/DSM) generated by photogrammetry with the UAV imagery. The classification between the ground and the vegetation was performed manually by visual inspection because the extent of the study site is small. Canopy models were also generated for every snow study site by differentiating the DSM from the DTM. Snow depth maps were generated using a snow surface model (DSM$_{snow}$) and compared to the DTM model to retrieve the snow depth for each spatial snow survey.

All covariates are raster data with an original spatial resolution below 0.1 m and were upscaled to a spatial resolution of 0.5 m. The final resolution of the spatial model is the same as the covariates. The choice of covariates is based on multiple studies that focus on spatial variation of snow depth. Three groups of covariates, terrain shape, vegetation and microclimate, are presented in Table 1. We choose two indicators to describe the terrain shape, the topographic position index TPI and the vector ruggedness measure. The topographic position index TPI is a slope descriptor indicating ridges, valleys or slopes at a given scale, it refers to the position in elevation relative to the neighbor cells (Weiss, 2001). The TPI is measured between a minimum radius and a maximum radius with weighted distance from the maximum radius(less important) (Table 1). The vector ruggedness measure indicates the ruggedness of the terrain independently of the slope and aspect. The ruggedness is derived with the sum of elevation differences with the neighbor cells, but then decoupled with the slope and aspect, meaning that a flat and a steep slope could be homogeneous with low ruggedness (Sappington J. Mark et al., 2007). These two indicators are widely used in the literature to explain and estimate the snow depth (e.g. Revuelto et al., 2020; Meloche et al., 2022; Veitinger et al., 2014). The sizes of the different moving windows were chosen based on the values used in these studies to have a multiscale approach (Table 1). We also used the slope of the terrain and also convexity as exploratory variables. Vegetation

Table 1. Covariates used for the spatial models with the source (DTM/DSM) and additional parameters.

Covariates	Abbr	Additional parameters	Processing library
Easting and northing	xy	NA	Python implementation
Terrain slope	Slope	NA	Qgis
Topographic Position index	TPI515	~~moving window~~ radius min/max = 5/15 m	SAGA ta-morphometry
Topographic Position index	TPI2550	~~moving window~~ radius min/max = 25/50 m	SAGA ta-morphometry
Vector ruggedness measure	VRM5	moving window = 5 m	SAGA ta-morphometry
Vector ruggedness measure	VRM15	moving window = 15 m	SAGA ta-morphometry
Vector ruggedness measure	VRM25	moving window = 25 m	SAGA ta-morphometry
Convexity	Convex	scale = 25	SAGA ta-morphometry
Canopy height	Cano	DSM/DTM	Qgis
Distance to canopy	Dist-cano	Radial proximity to trees > 2 m	SAGA grid tools
Incoming solar radiation	Rad	Hourly time steps 30 days before sampling	SAGA ta-lighting
Snow depth	H_s	$DSM_{snow} - DTM$	Qgis
Winstral index	S_x	Search ~~radius~~ distance = 100 m	Python Winstral et al. (2002)

300   also has an impact on the spatial variation of snow depth (Deems et al., 2006), we choose to use the canopy height ~~and also the~~
for the influence of shrubs (around 0.3 and 0.5 m) and small trees (around 1 or 2 m) because the snowpack can be up to 3 or 4 m
in some areas in JBC and RH. Only trees above 5m were masked from the study sites. We use the radial proximity to vegetation
greater than 2 m, to represent proximity to trees. Some authors also found that solar radiation (e.g. Lutz and Birkeland, 2011)
and wind exposure (e.g. Winstral et al., 2002) were important to spatially estimate snow properties. We selected as covariates

305   the potential of incoming solar radiation, ~~using a DSM to represent the shading and the sunshine area~~ the algorithm simulates
over a DSM, the trajectory of the sun in the sky based on the ~~Sun trajectory over a DSM in a time period~~ time of the year and the
latitude of the study site. The covariate represents direct insolation (shade and sunshine areas), calculated over a month prior
to the survey. The Winstral index or upwind maximum slope parameter S_x ~~(Winstral et al., 2002) described the wind exposure~~
~~in a DSM~~ represents the shelter or exposure areas provided by the terrain upwind of each pixel (Winstral et al., 2002). The

310   upwind terrain is defined with the maximum search distance and the prevalent wind direction based on the ~~dominant wind~~
~~direction~~ mean wind direction from the nearest weather station of the study sites over the winter. The last ~~covariates used were~~
covariate used was the spatial coordinates (easting and northing). The fitting of a smooth function, explained below, to spatial
coordinates will take into account the residual spatial autocorrelation (Nussbaum et al., 2017). The processing of the covariates
is described in Table 1, using the geoprocessing library SAGA (Conrad et al., 2015), Qgis 3.14, and a python implementation

315   of the Winstral index S_x according to Winstral et al. (2002).

2.5.2 General additive model

General additive models (GAMs) can represent ~~nonlinear~~ non-linear relationships between the covariates and the response variable. GAMs have been used in the past for spatial estimation of environmental variables (Nussbaum et al., 2017). They produce good results while remaining easy to interpret compared to more complex tree classification methods and machine learning algorithms (Nussbaum et al., 2017). A GAM model can be described as a generalized linear model with a linear prediction involving a sum of smooth functions of covariates (Wood, 2006):

$$g[K(Y_i)] = X_{*}i\theta + s_1(x_1i) + s_2(x_2i) + s_3(x_3i) + ...s_j(x_ji) \tag{12}$$

where g is a link function to a family distribution, Y_i is a response variable from some exponential family distribution K, X_i is a row of the model matrix for any strictly parametric component with vector parameter θ. Each smooth function or spline s_j can be expressed by a basis expansion b with a weight parameter β and k defining the order of the basis expansion.

$$s_j(x_j) = \sum_{k=1}^{k} \beta_k b_k(x_j) \tag{13}$$

Each smooth function represents a combination of linear terms fitted to a covariate x_j. The order of the smooth function defined the non-linear degree or the *wigliness* of the fitted GAM. We choose to keep the order low ($k = 3$) to avoid overfitting and non-realistic variation. Although stepwise procedures are widely used, they lack stability compared to newer methods such as shrinkage and boosting procedures (Hesterberg et al., 2008). We choose to use the double penalty approach as a shrinkage method proposed by Marra and Wood (2011). This method adds a smoothing parameter for each covariate spline function. This method is implemented in the package *mgcv* in R. ~~Once our model is fitted and the covariates are selected, we estimated the response variable for every location at each study site on a 0.5 m resolution grid. Finally, the~~ We repeated this method for six response variables, the three snow mechanical properties, the slab thickness D, slab density ρ_{slab} and the shear strength of the weak layer τ_p, and also the three stability metrics described above, which are the skier crack length l_{sk}, the critical crack length a_c and the skier propagation index SPI. These response variables were estimated with GAM's using the 13 covariates listed in Table 1. The performance of our models was assessed with the root mean square error RMSE and the mean absolute error MAE using a 10-fold cross-validation approach. This procedure splits the sample randomly ~~in~~ into 10 subsets and fits the model to the 9 subsets and compares it to the remaining subset, this procedure is repeated 10 times. The ~~computation was done~~ percentage of deviance explained (sum of squared errors) is computed to demonstrate the amount of total variance accounted by the model, this metric is more suited for non-linear model compared to R^2, which is still shown in the results for comparison. Once our model is fitted (and cross-validated) and the covariates are selected, we estimate the response variable for every location at each study site on a 0.5 m resolution grid. A smaller resolution will not be in line with the assumption of homogeneous snowpack for the computation of the skier crack l_{sk} and the critical crack length a_c. All statistical computations were performed in R (R Core, 2013).

Table 2. Summary for the snow measurements of all four spatial surveys. The results of the compression test CT results and the propagation saw test PST are shown according to the standards of Canadian Avalanche Association (2016).

Surveys	Date	Mean D & ρ	Weak layer	Nb SMP	Extent	CT	PST (m)
AR22-PP	2022-02-25	0.28 m & 252 kg m^{-3}	PP 0.5-1 mm	45	71 m	CTM11 (RP) down 0.25 m	0.9/1.5 END
						CTH23 (RP) down 0.54 m	1.42/1.5 END
						CTH22 (RP) down 0.35 m	1.22/1.5 END
RH22-PP	2022-01-27	0.19 m & 171 kg m^{-3}	PP 0.5-1 mm	64	116 m	CTM19 (RP) down 0.22 m	0.8/1.5 END
						CTM19 (RP) down 0.22 m	0.28/1.5 SF
						CTH22 (RP) down 0.24 m	1.38/1.5 END
JBC22-SH	2022-01-19	0.39 m & 188 kg m^{-3}	SH 1-2 mm	53	102 m	CTH21 (RP) down 0.39 m	1.28/1.5 END
						CTM12 (RP) down 0.5 m	1.46/1.5 END
JBC22-PP	2022-01-24	0.21 m & 166 kg m^{-3}	PP 0.5-1 mm	55	74 m	CTM13 (RP) down 0.25 m	1.24/1.5 END
						CTM16 (RP) down 0.24 m	1.41/1.5 END
EP20-DF	2020-02-29	0.32 m & 241 kg m^{-3}	DF 0.5-1 mm	38	45 m	CTH23 (RP) down 0.38 m	-
						CTH24 (RP) down 0.45 m	-
EP19-FC	2019-01-24	0.85 m & 333 kg m^{-3}	FC 1 mm	22	48 m	CTH20 (SP) down 0.82 m	-
						CTM22 (RP) down 0.88 m	-

3 Results

3.1 Summary of spatial snow surveys

The first spatial snow survey is at the AR site. A weak layer of precipitation particles ~~between~~ with an observed grain size of 0.5 - 1 mm was investigated on 25 February 2022 (AR22-PP), with 45 SMP measurements and a spatial extent of 71 m. The slab thickness was on average 0.28 m with a high mean density of 252 kg m^{-3} (Table 2). This study site is highly wind-affected, especially in the upper part of the slope with a higher slab density. The bottom of the slope is more protected from the wind, whereas the slab is softer with a lower density. At the RH site, a weak layer of precipitation particles with an observed grain size of between 0.5 and 1 mm beneath a relatively fresh and soft snow slab, with a mean slab thickness of 0.19 m and a mean density of 171 kg m^{-3}. This survey was done on 27 January 2022 with 64 SMP measurements and a spatial extent of 116 m. The slab for this survey is made up of one layer of homogeneous storm snow, and both the slab and the weak layer are from the same meteorological event. We were able to conduct two spatial snow surveys at the JBC site in two different areas of the site. The first survey at this site was done on January 19, 2022 (JBC22-SH) when there was a weak persistent layer of buried surface hoars of size 1-2 mm. The slab is composed of multiple layers, given a mean slab thickness of 0.39 m and a mean density of

188 kg m^{-3} above the surface hoar crystals. This survey ~~is made up~~ consists of 53 SMP measurements and a spatial extent of 102 m. The second field survey was carried out ~~on~~ in a snowpack characterized by a weak layer of precipitation particles buried under a fresh snow slab of 0.21 m and 166 kg m^{-3} on average, which comes from the same meteorological event as RH22-PP. This survey was carried out on 24 January 2022 (JBC22-PP) with 55 SMP measurements and a spatial extent of 74 m (Table 2).

~~Summary for the snow measurements of all four spatial surveys. The results of the compression test CT results and the propagation saw test PST are shown according to the standards of Canadian Avalanche Association (2016). Surveys Date Mean slab~~ Figure 3 demonstrates slab density ρ and the weak layer shear strength in relation to slab thickness D ~~&~~ . These relations are well defined in snow science, as the snow density and the snow strength should increase as the snow weight increases. Figure 3 shows our data set compared to two empirical power law fits (Bažant et al., 2003; McClung, 2009a), which are used to parameterize realistic snow mechanical values in relation to the slab thickness. Two other power laws were fitted to the slab density ρ ~~Weak layer Nb SMP Extent CT a_c PSTAR22-PP 25-02-2022 0.28 m & 252~~ and weak layer shear strength τ_p. Figure 3-a agrees well with our 'softer-slab' surveys ($\rho < 250$ kg m^{-3} ~~PP 0.5-1 mm 45 71 m CTM15 RP @down 0.25 m 1.11 m RH22-PP 27-02-2022 0.19 m & 171~~) conducted at Mount Fidelity, but could easily be adjusted by increasing the initial density in the power law for the survey where the mean density is higher. Surveys with higher density ($\rho > 250$ kg m^{-3} ~~PP 0.5-1 mm 64 116 m CTM19 RP @down 0.22 m 0.8 m JBC22-SH 19-01-2022 0.39 m & 188 kg m^{-3} SH 1-2 mm 53 102 m CTH21 Brk @down 0.39 m 1.28 m JBC22-PP 24-01-2022 0.21 m & 166 kg m^{-3} PP 0.5-1 mm 55 74 m CTM13 RP @down 0.25 m 1.24m~~) were on Mount Albert, which is a heavily wind-exposed area that could explain these highly dense slabs. Figure 3-b shows some surveys align well with the two power laws, especially the surveys from Mount Fidelity (circles). The "stronger" surveys (crosses) from Mount Albert could also be fitted if the initial cohesion is increased. However, the Mount Albert surveys contained more variability compared to the Mount Fidelity surveys. Our dataset demonstrates that, in general, our data set fits approximately the power-law fits, but a lot of variability remained in each survey. The intra-survey variability and implication for snow mechanical modeling will discussed in section 4.1.

3.2 Comparison of spatial patterns

For all spatial snow surveys, the empirical variogram showed smaller correlation lengths for the slab thickness compared to other properties, ranging from 5 to 10 m (Fig. 4). The slab density variograms were also small and similar to the slab thickness variogram for JBC22-PP and RH22-PP, with 5 and 8 m respectively. These two spatial snow surveys had the same weak layer and slab meteorological deposition event characterized by a new snowfall instability. The correlation length for AR22-PP is 10 m, with the same type of new snowfall instability. The last one at the Jim Bay corner (JBC22-SH) has longer correlation lengths of around 20 to 30 m. The empirical variogram for this survey shows a correlation around 20 m, but shows significant variability that makes the estimation less reliable compared to the other empirical variograms (Fig. 4). The variogram of the slab density from JBC22-SH, JBC22-PP and AR22-PP also had fractal characteristics with a stabilization of the variance around 20 m, followed by an increase in variance around 30 and 40 m. If we look at the variogram of the shear strength of the weak layer, the four spatial snow surveys had a longer correlation length around 20 m compared to slab properties which are
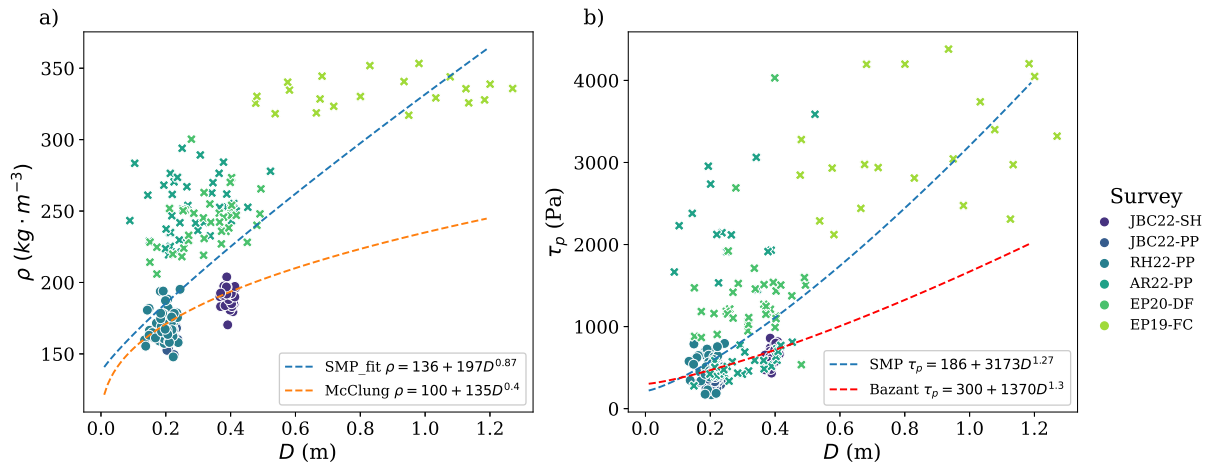
Figure 3. SMP derived slab density ρ_{slab} (a) and weak layer shear strength τ_p (b) in relation to the slab thickness D for each SMP measurement of all spatial survey. The circles represent the SMP values in Mount Fidelity, British Columbia, and the crosses are from the surveys in Mount Albert, Québec. A power law in blue was fitted to the SMP-derived values of all the surveys, with, respectively, a) 0.5 R^2 for ρ and b) 0.4 R^2 for τ_p. a) The orange power law fit represents ρ compared to D, with an initial density of 100 kg m^{-3} from McClung (2009a). b) The red power law is the power law for τ_p from Bažant et al. (2003) reported to Mohr-Coulomb criterion with an initial cohesion of 300 Pa (Gaume et al., 2014).

around 10 m. The JBC22-PP and RH22-PP surveys, the same meteorological deposition event, had a variance stabilized at 20 m without any further increase in variance. The other surveys (JBC22-SH and AR22-PP) had longer correlation lengths and

395   ~~show~~ showed fractal characteristics with no stabilization in variance with increasing sampling distance. The type of variogram models that were fit was mostly spherical ~~, characterized by~~ and exponential, which exhibit a rapid increase in variance for small distances. ~~Gaussian models were also~~ These models are typically less smooth than Gaussian models (smaller variance for short distances), which were fitted for slab thickness at JBC22-SH and slab density at JBC22-PP ~~, characterized by stable variance for short distances followed by an increase~~. However, these two fitted Gaussian models still showed a shorter correlation (>

400   5 m). In general, the correlation lengths are ~~smaller~~ shorter for the thickness and density of the slab compared to the shear strength of the weak layer ~~,~~ for each snow spatial survey.

At first glance, all the correlation lengths for the stability metrics are around 20 m, thus longer than the slab properties. Surveys at the Jim Bay corner (JBC22-SH and JBC22-PP) had smaller correlation lengths of around 20 m compared to the other two surveys with longer correlation lengths of around 30-40 m (Fig. 5). The same similarity can be observed for the

405   correlation length of the critical crack length and also for the skier index. The skier index is the ratio between the critical crack length and the skier crack length, so this result is quite expected. The correlation length of the stability metrics is around 10 to 20 m, but some are around 30 to 40 m, which is quite large compared to the slab properties (Fig. 5). The variogram model used is mostly spherical, but also ~~gaussian for the slab thickness~~ Gaussian for the skier crack length (JBC22-PP, RH22-PP, AR22-PP) and skier index (JBC22-SH, JBC22-PP). Gaussian models were fitted more to stability metrics than snow properties, showing
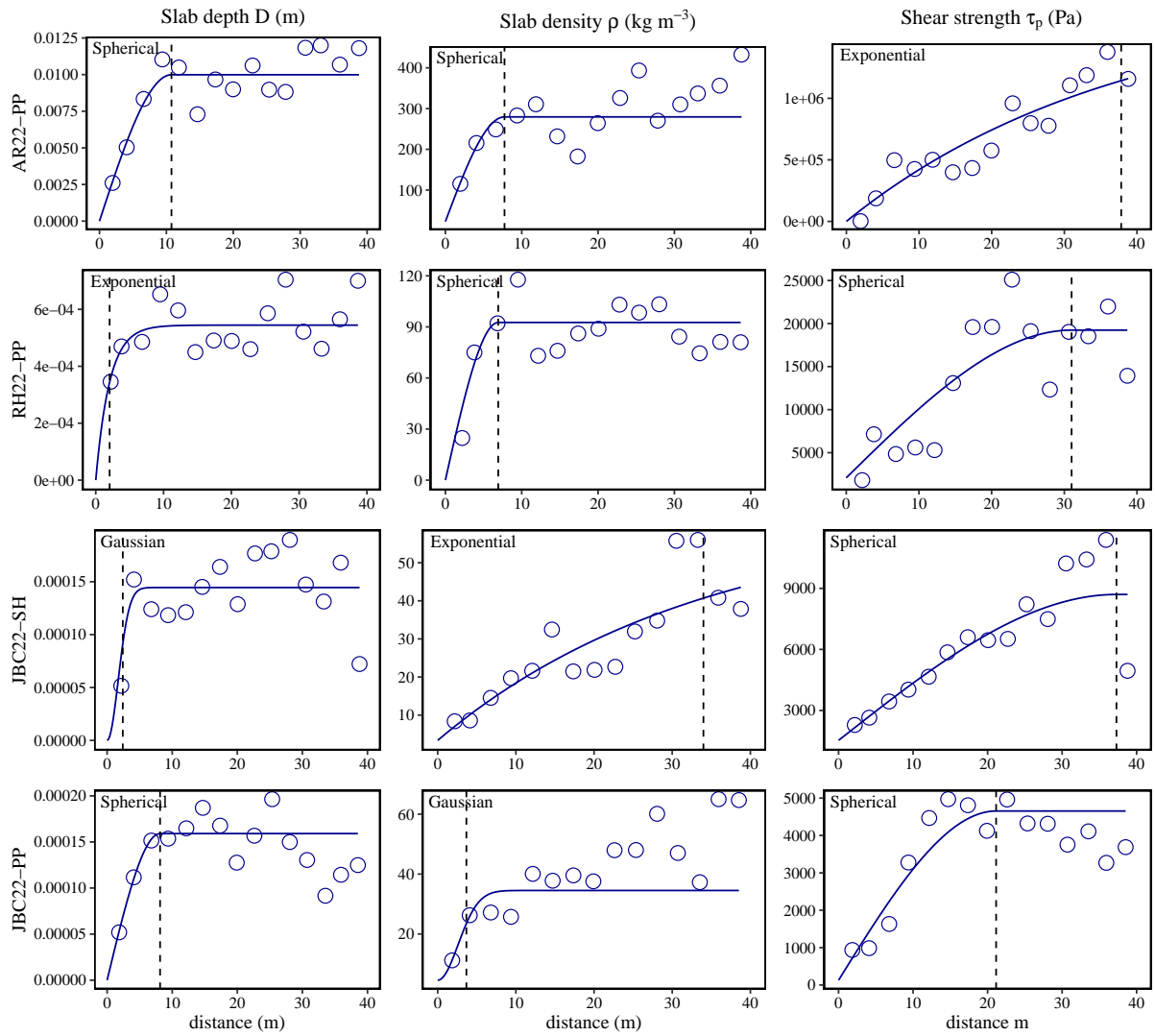
Figure 4. Experimental variogram (circles) and fitted variogram models (line) for the snow mechanical properties. Note that the square root of the variance gives the absolute variation.
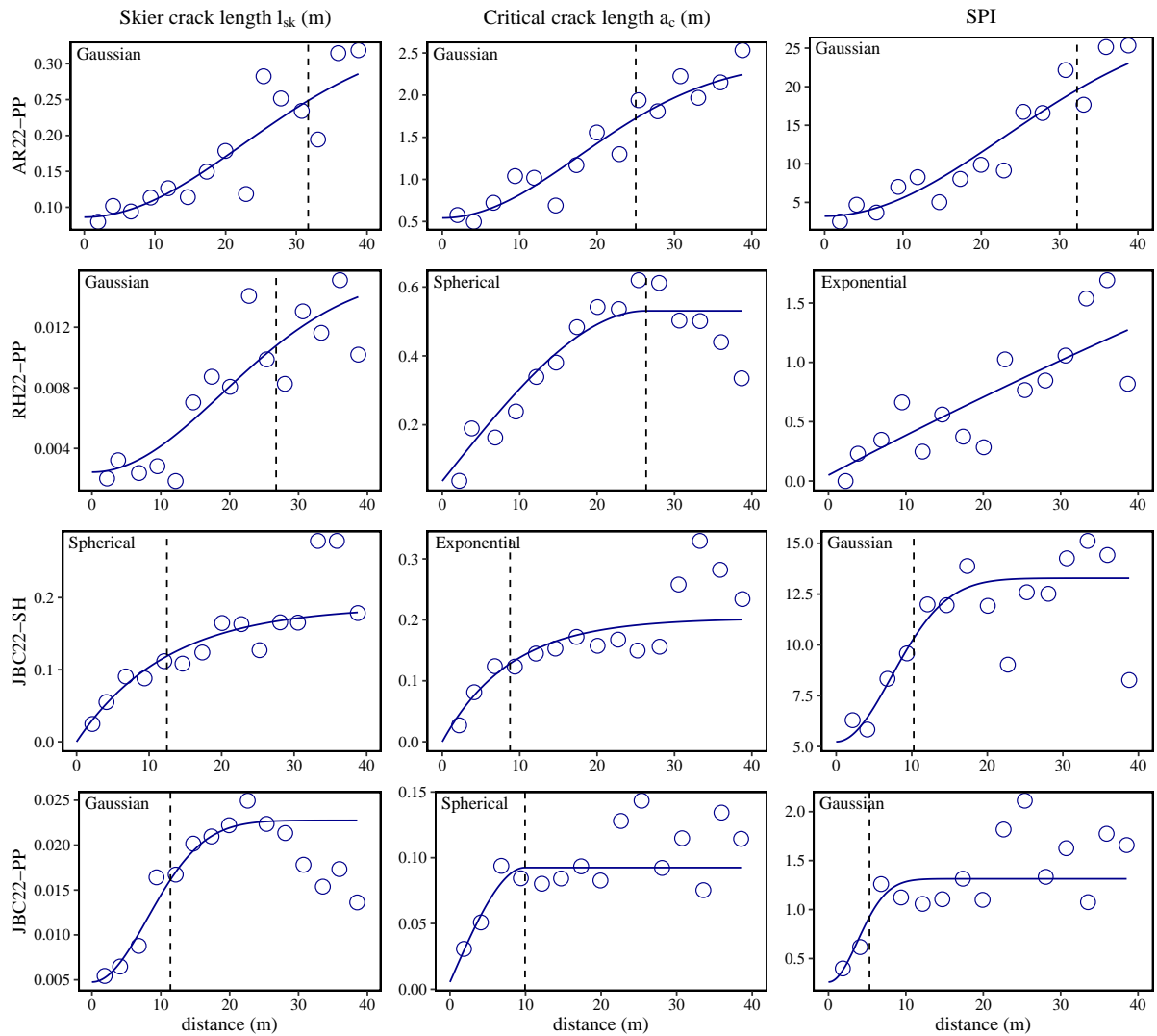
Figure 5. Experimental variogram (circles) and fitted variogram models (line) for the stability metrics. Note that the square root of the variance gives the absolute variation.
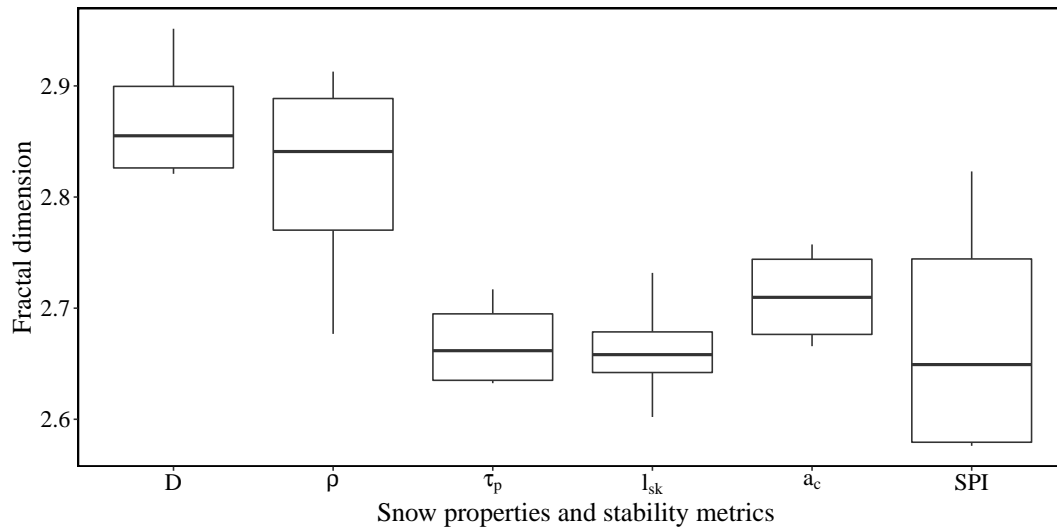
Figure 6. Boxplot of fractal dimension for snow mechanical properties and stability metrics with the four surveys in each boxplot.

smoother spatial patterns for the stability metrics. The variogram for the stability metrics shares more similarities with the variogram of the weak layer shear strength rather than the slab properties.

The fractal dimensions for the snow properties showed a difference in surface roughness or complexity between the slab properties, the weak layer properties, and the stability metrics (Fig. 6). The slab properties have higher fractal dimensions of around 2.85, thus a higher surface ~~roughness~~complexity, compared to the weak layer and the stability metrics, which yield a similar fractal dimension of around 2.7. The values for the stability metrics are computed from the slab mechanical properties and weak layer properties, but the values of fractal dimension seem to be in the same range as those for the weak layer rather than the slab. These results suggest that the spatial patterns of the stability metrics are more similar to the spatial pattern of the weak layer than to the spatial pattern of the slab properties.

3.3 Spatial modeling

The spatial models created by GAMs were able to explain some of the variance of the response variable, but not entirely. The R^2 and the percentage of deviance explained range from 0.17 to 0.84 and from 22 to 84 % (Table 3 - 4). As for the average, it is approximately around 0.5 and 55 %. The average R^2 is 0.47 for snow properties and 0.55 for stability metrics, but the average percentage of deviance explained is the same at 55 %. The performance of the models was assessed with a 10-fold cross-validated RMSE and MAE. The cross-validated RMSE and MAE for the slab thickness D were mostly 1-2 cm except for 12 cm at AR22-PP and were around 4 to 27 kg m^{-3} for the slab density. The RMSE and MAE for the shear strength range from 30 to 128 Pa except for 752 Pa for AR22-PP, but this snow spatial survey was also the one with the more variance (500 to 3500 Pa).

Table 3. Summary of the spatial models, model selection, and performance metrics for the snow properties. The performance metrics are the following R^2, the percentage of deviance % dev, scale, the cross-validated Root-mean-squared-error CV RMSE, and the cross-validated mean-absolute-error CV MAE. The symbols next to the covariates refer to the significance levels of the p-value: > 0.1 ".", < 0.05 "*", < 0.01 "**", < 0.001 "***".

Site	Snow prop.	Covariates	R^2	% dev	scale	CV RMSE	CV MAE
JBC22-SH	D	TPI2550* + VRM25 + VRM5* + H_s* + Convex. + Dist-cano* + S_x*	0.35	42.9	9.57e-5	0.01	0.01
JBC22-SH	ρ_{slab}	Slope** + VRM15*** + H_s* + Convex*** + Dist-cano*	0.57	64.1	12.22	7.91	4.78
JBC22-SH	τ_p	(x+y)* + Slope* + TPI515* + VRM15** + VRM5* + Convex* + Cano.	0.50	66.2	3762.3	66.29	51.70
JBC22-PP	D	VRM5. + Cano*	0.17	22.2	0.0001	0.01	0.01
JBC22-PP	ρ_{slab}	Slope** + TPI515** + TPI2550*** + VRM25** + VRM15** + VRM5* + H_s. + S_x.	0.64	69.6	15.13	6.32	5.00v
JBC22-PP	τ_p	(x+y)*** + TPI2550*** + VRM25** + VRM15 + VRM5*** + Dist-cano** + S_x*	0.76	80.4	864.78	41.32	30.79
RH22-PP	D	(x+y)*** + Slope* + TPI515*** + TPI2550* + Cano** + Dist-cano** + S_x**	0.54	60	0.0002	0.03	0.02
RH22-PP	ρ_{slab}	(x+y)** + Slope. + TPI515. + VRM15** + Convex*** + Cano*	0.32	38.2	64.99	11.39	8.51
RH22-PP	τ_p	(x+y)** + TPI2550*** + VRM25* + VRM5** + Rad* + Cano**	0.42	48.3	10463	128.37	99.70
AR22-PP	D	(x+y). + VRM15* + VRM5. + Cano.	0.28	36.2	0.006	0.12	0.10
AR22-PP	ρ_{slab}	(x+y)** + TPI2550. + H_s. + Convex**	0.41	46.8	216.77	21.78	21.80
AR22-PP	τ_p	(x+y)*** + Slope* + TPI2550*** + VRM5* + Convex*** + Dist-cano*	0.72	76.7	2.157e5	752.70	578.88

The spatial surfaces estimated by the GAM models in JBC22-SH for the snow mechanical properties are presented in Figure 7. The estimated surface for the slab thickness and density had ~~the same~~ a similar variation with the same maximum and minimum areas. The estimated surface for the shear strength of the weak layer differs slightly from the slab properties. ~~The areas of maximum and minimum values are not necessarily in the same areas as the slab properties, but the main areas of maximum and minimum values are relatively the same as the slab properties.~~ This result also reinforces the above results, showing that the spatial pattern of the weak layer differs from the slab properties in our dataset. Estimation errors for critical crack length are around 0.11 to 0.60 m, except for 1.2 m for AR22-PP. The RMSE and MAE for the skier propagation index ranged from 0.27 to 4, which is very variable and quite high for an index. The estimation errors for the stability metrics

Table 4. Summary of the spatial models, model selection and performance metrics for the stability metrics. The performance metrics are the following R^2, the percentage of deviance % dev, scale, the cross-validated Root-mean-squared-error CV RMSE, and the cross-validated mean-absolute-error CV MAE. The symbols next to the covariates refer to the significance levels of the p-value: > 0.1 ".", < 0.05 "*", < 0.01 "**", < 0.001 "***".

Site	Stab. metrics	Covariates	R^2	% dev	scale	CV RMSE	CV MAE
JBC22-SH	l_{sk}	(x+y)* + Slope** + VRM15*** + VRM5. + Convex.	0.58	64.8	0.06	0.48	0.22
JBC22-SH	A_c	Slope*** + TPI515** + TPI2550* + VRM15*** + VRM** + H_s***	0.60	65.9	0.06	0.20	0.14
JBC22-SH	SPI	Slope** + VRM15* + VRM15** + H_s*	0.35	40.3	6.66	2.5	1.89
JBC22-PP	l_{sk}	(x+y)*** + TPI2550** + VRM25** + VRM5** + S_x*	0.60	65.1	0.006	0.10	0.07
JBC22-PP	A_c	(x+y)* + TPI515*** + VRM5*** + H_s. + Rad** + S_x*	0.74	77.7	0.02	0.15	0.11
JBC22-PP	SPI	(x+y)** + TPI515*** + VRM5*** + Rad** + S_x*	0.84	87	0.20	0.36	0.27
RH22-PP	l_{sk}	(x+y)*** + TPI2550** + VRM25** + VRM15* + VRM5* + Rad* + Cano*	0.51	57.1	0.004	0.11	0.08
RH22-PP	A_c	VRM25** + VRM5**	0.25	28.7	0.39	0.60	0.47
RH22-PP	SPI	(x+y)*** + VRM25*** + Rad. + Convex**	0.43	48.5	0.61	1.23	0.85
AR22-PP	l_{sk}	(x+y)** + VRM25*	0.22	27.5	3.2	2.97	1.85
AR22-PP	A_c	TPI2550*** + VRM15* + Convex* + Cano. + S_x.	0.65	69.1	0.61	1.26	1.01
AR22-PP	SPI	TPI2550*** + Convex**	0.66	68.7	5.14	4.29	3.31

were high and not reliable compared to the snow mechanical properties. However, Figure A1 shows that ~~the RSME might be overestimated by some outliers~~ some outliers might overestimate RSME with low values of l_{sk} and high SPI values (SPI ≈ 10). The spatial patterns of the stability metrics indicate ~~2~~ two major weak spots on the north side (right) and northwest (upper-middle). These weak spots correspond to areas with lower shear strength values and slightly thicker and higher-density slabs.

440   There are no clear covariates ~~that are used~~ selected by the model for every site, snow properties, or stability metrics. However, some covariates were used more often than others. The most used covariates for both snow properties and stability metrics were multiscale TPI and VRM, but their usage is quite variable depending on the scale (Fig. 9). The shear strength of the weak layer appeared to use mainly TPI2550 and VRM5 compared to the slab density, which used mainly VRM15 and convexity. The

445   canopy height was used in the snow properties models but not really in the stability metrics models. The easting and northing coordinates were widely used in the models showing the presence of autocorrelated residuals. Surprisingly, snow depth was not used as much as other covariates. These results showed that there are no universal covariates or specific covariates for snow
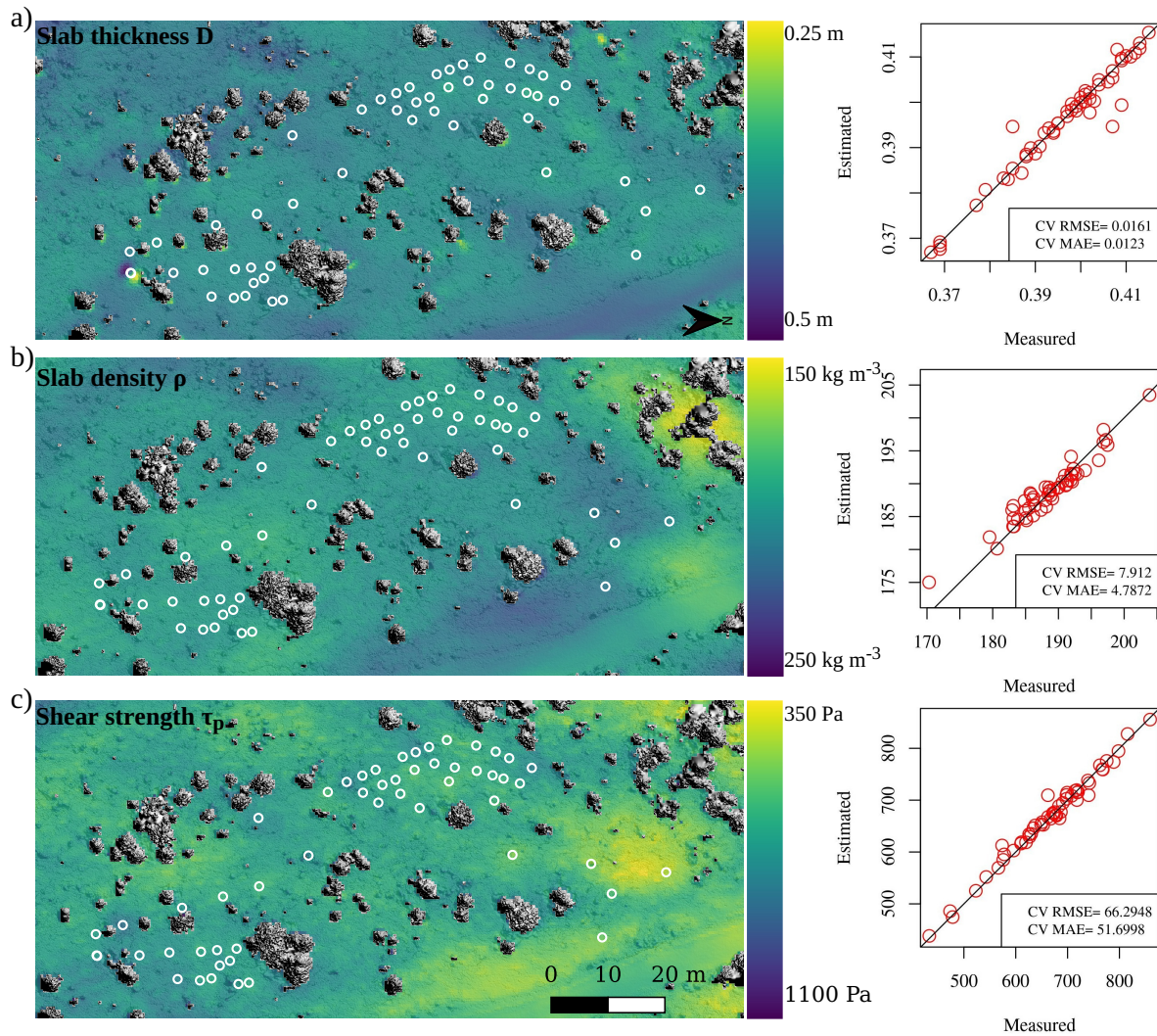
Figure 7. Spatial estimation for the snow mechanical properties a) slab thickness D, b) slab density ρ, c) shear strength τ_p at the Jim bay corner on 19 January 2022 (surface hoar layer - 1mm). The cross-validated root mean squared error RMSE and the mean absolute error MAE are shown next to the map of each property. The grey shading in the background map represents a canopy shading only for the visualization of trees.

properties or stability metrics. However, these results demonstrate the utility of using these covariates to spatially estimate the snow properties, and also stability metrics with less precision.
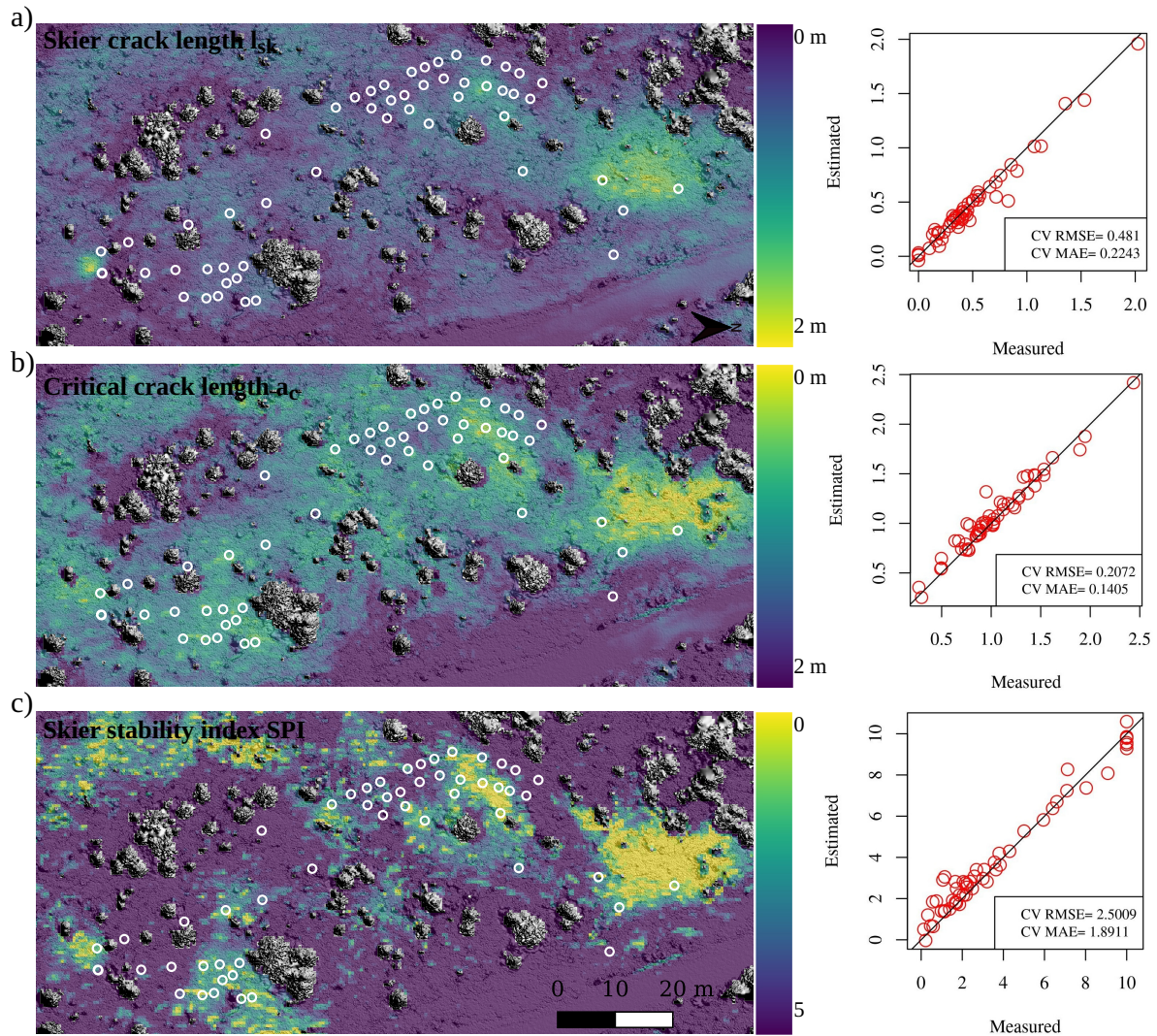
Figure 8. Spatial estimation for the stability metrics a) skier crack length l_{sk}, b) critical crack length a_c, and c) Skier propagation index SPI at the Jim bay corner on 2022-01-19 (surface hoar layer - 1mm). Cross-validated root mean squared error RMSE and mean absolute error MAE are shown next to the map of each metric. The grey shading in the background map represents a canopy shading only for the visualization of trees.
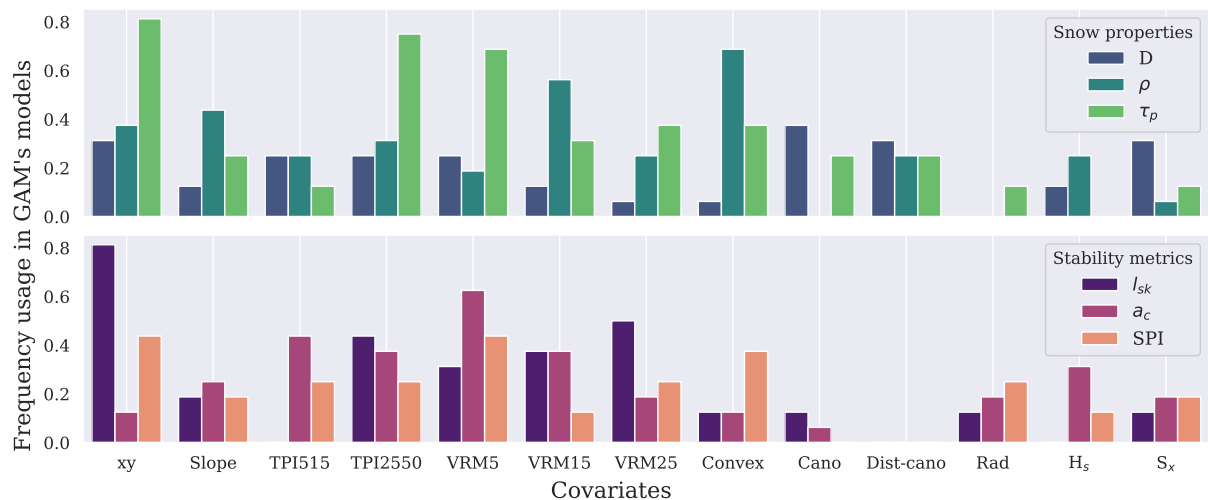
Figure 9. The frequency usage of covariates in the GAM spatial models, the frequency is ~~pondered~~ weighted with the significance levels of the p-value.

4 Discussion

4.1 Spatial modeling

This study gathers a unique dataset describing the spatial variation of snow mechanical properties and stability metrics at four different study sites. The comparison of the variograms and fractal dimensions demonstrates that the slab properties (depth and density) vary at a different scale compared to the weak layer properties and stability metrics (smoother pattern). Spatial GAM modeling was used to spatially predict with good accuracy the snow mechanical properties using microtopography and with less precision the stability metrics. However, Our spatial modeling did not fully explain the variance of each response variable. Some spatial ~~variance could~~ variances remain unexplained, but ~~it~~ could also be attributed to ~~a nonspatial variance~~ non-spatial variances, such as instrument error or our processing data strategy. This strategy includes a visual interpretation of the layer in the SMP resistance profile. A misclassification or misidentification of the weak layer boundaries can influence our results by adding non-spatial variance to our dataset. However, we used the SMP parameter L in the parameterization F_{wl} proposed by (Richter et al., 2019) instead of the thickness of the weak layer for the computation of the critical crack length (Gaume et al., 2017). This modification makes our method less dependent on the weak layer thickness, which was visually identified for each SMP profile. The RMSE was still quite high for the stability metrics and, thus less reliable for spatial estimation purposes. The SPI values were quite low (~~>~~<0.5) for some areas in the spatial survey. If we had sampled these areas walking with the SMP, these areas should have been triggered, but nothing happened. This indicates that the stability metrics estimations are too pessimistic. We are not sure where the error might be, maybe in the SMP processing or the spatial modeling, or maybe both. However, the cross-validated RMSE for the snow mechanical properties was good with reliable precision according to the properties (Table 3), indicating that the SMP processing for the snow mechanical properties is good, as well as the

GAM spatial modeling compared to the stability metrics. Future work could use spatial estimations of the snow mechanical
470   properties to compute the stability metrics from the spatial field of snow properties. The cross-validation procedure is performed
by randomly selecting 10 subsets. The random selection could take into account a minimum distance between observations
(i.e our correlation length) to ensure complete independent subsets before computing the RMSE and MAE, and could bias the
estimation of the RMSE and MAE However, our 10-fold cross-validation (repeated 10 times) still provides a reliable estimation
of the performance of our models. Future work should take this into account.

4.2   Microtopographic covariates

This study aimed to use microtopographic covariates to spatially predict snow spatial variation and stability. Our GAM spatial
modeling did not reveal a universal covariate that predicts both snow mechanical properties or stability metrics. The study of
Reuter et al. (2016), based on larger-scale terrain-based covariates, did not find a universal covariate to predict instability at
the basin scale. They reported that the slope aspect was selected as a predictor by the model in all of their surveys, but each
480   survey used a different combination of covariates. Like the study of Reuter et al. (2016), the selection of covariates was specific
to each survey with no clear trend or takeaway regarding the choice of covariates. Surprisingly, snow depth was not a good
estimator of snow mechanical properties and stability metrics~~for our dataset. Slope seems to be a better spatial estimator for
snow instability. The~~ . Reuter et al. (2016) also reported that all their terrain-related covariates were used in 7 of their surveys,
but snow depth was only in six of them. In our study, snow depth was only used to predict slab depth and slab density but
485   the model never selected snow depth to predict the shear strength of the weak layer. A possible explanation could be that
the weak layer spatial variation is not related to the snow accumulation process, or that our dataset was too homogeneous
regarding snow depth. AR22-PP is a wind-exposed study site and, surprisingly, the GAM model did not select the Winstral
index S_x as good predictor. The research distance in S_x represents the scale of the indicator and the one selected in the study
might be too large (100 m). Using multiple scales like in the case of TPI and VRM, could change S_x as a significant covariate
490   at the wind-exposed site (AR22-PP). Unfortunately, no link could be made between our only persistent weak layer survey
(JBC22-SH) and the remaining non-persistent weak layer surveys. A bigger dataset is needed to demonstrate clear differences
between alpine/forested areas and persistent/non-persistent weak layers. The covariates TPI and VRM are the best covariates
for estimating snow properties, ~~also in accordance with~~ this was also observed by previous studies using spatial models ~~to~~
~~(random forest) to spatially~~ estimate snow depth (Meloche et al., 2022; Revuelto et al., 2020). The best scale, or window size,
495   of TPI and VRM for prediction seems to be changing depending on the study site, snow properties and stability metrics. Future
work with a larger dataset should investigate if the best scale is related to the specific scale of the terrain at each site, the scale
of the meteorological process affecting the slab and the weak layer, or interaction with both. Still, the multiscale covariate TPI
associated with ~~the terrain shape seems~~ terrain shape appears to be a good spatial estimator for backcountry recreationists.
VRM could also be a good estimator for backcountry recreationists, but it ~~might~~ could be more difficult to identify with ~~a~~
500   snow-covered terrain. Weak layer spatial variability remains the main information ~~to monitor for~~ for monitoring the spatial
occurrence of snow instability~~but it is difficult to assess quickly on the~~ , but the difficulty of quickly assessing the weak layer
spatial pattern in the field for backcountry recreationists remains a challenge.

4.3 Snow mechanical parametrization and modeling

505 Our study agrees with the well-known relationship between the slab thickness and the slab density due to snow settlement. Our results also show The comparison of the spatial pattern between surveys shows that these two properties exhibit the same spatial pattern in the variogram, the fractal dimension, and their covariates used for spatial modeling. For further study, the empirical power-law fit $\rho \sim 100 + 135D^{0.24}$ suggested by McClung (2009b) $\rho \sim 100 + 135D^{0.4}$ suggested by McClung (2009a) is a good way to easily represent the interaction between these two properties to obtain realistic snow values for mechanical

510 simulation (e.g. Gaume and Reuter, 2017). Figure 3 agrees well with our 'softer-slab' surveys ($\rho < 250$ kg m^{-3}) conducted at Mount Fidelity, but could easily be adjusted by increasing the initial density in the power law relation for the survey where the mean density is higher. The surveys with very high density ($\rho > 250$ kg m^{-3}) were on Mount Albert, which is a heavily However, our SMP power law fit could be better represent denser slabs in wind-exposed area that could explain this result caused by these really dense slabs areas. The power-law fit could also be used to generate the slab density based on the spatial

515 pattern of the slab thickness if some variation is included in the simulation. Thus far Until now in snow mechanical modeling, the spatial variation of snow properties was limited to the weak layer. Our study shows that there is a difference between the spatial variation of the slab properties and the slab weak layer in our dataset. This difference was previously observed by Bellaire and Schweizer (2011), in their spatial survey to conduct over a smaller extent. Our study shows the need to account for both slab properties variation and weak layer variation because spatial patterns can differ from each other.

520 Our results show study shows that the weak layer variation was smoother than the slab and the increase in shear strength did not necessarily match the increase in the slab thickness. In general, shear strength should increase with slab thickness due to the slab weight, but some variation was still present in our dataset (Figure 3). The interaction between slab thickness and shear strength can be described with a power law $\tau_p \sim c + 1370D^{1.3}$ (Bažant et al., 2003), but it was reported according to the Mohr-Coulomb criterion with initial cohesion c (Gaume et al., 2014). Figure 3 shows our SMP dataset with this power law relation

525 between τ_p and D. Some surveys are well aligned with this power law, especially the surveys from Mount Fidelity (circles). The "stronger" surveys (crosses) from Mount Albert could also be fitted if the initial cohesion is increased. However, the Mount Albert surveys contained more variability compared to the Mount Fidelity surveys. Figure 3 shows two power law fits taken from the literature with our SMP dataset. (300 Pa in Figure 3) (Gaume et al., 2014). These power laws could represent well the average values of the survey from Mount Fidelity, the average value of Mount Albert but our fitted power laws could also

530 be represented if the initial values were increased used for thicker (denser) slabs in wind-exposed areas. However, these power laws did not adequately capture the variability in values for a specific spatial survey. The constant parameters need parameter needs to be adjusted for every spatial survey to fit the values. These power laws could be used to estimate the average snow values if only the slab thickness is available, but a stochastic process could be added to generate a more realistic variability.

Gaume et al. (2013) proposed a method to generate a weak layer with spatial heterogeneity. The method generates a random

535 field with a specified mean, variance, and correlation length for the cohesion of the weak layer in the Mohr-Coulomb relation. The friction term of the Mohr-Coulomb, which incorporates the slab thickness, is added to the cohesion to obtain the shear

strength. Their fiction term was constant because the slab thickness was constant, but this method could easily be adapted with a variable friction term following a variation in the thickness of the slab. These methods would allow two different random fields to be specified for both the properties of the slab and the weak layer while respecting the friction regarding the slab thickness. This method still needs a mean, variance, and correlation length as input. The empirical power law can estimate mean values, but according to our dataset, the variance is not well represented (Fig. 3). Future work should explore the possibility of estimating the variance and the correlation length using the covariance of microtopography combined with the snow cover model outputs. These methods could lead to more realistic simulations in avalanche modeling for forecasting purposes, both for the probability of skier triggering and the avalanche release size.

~~SMP derived ρ_{slab} and τ_p in relation to the D for each SMP measurement of all spatial survey. The circles represent the SMP values in Mount Fidelity, British Columbia, and the crosses are from the surveys in Mount Albert, Québec. A power law in blue was fitted to the SMP-derived values of all the surveys, with, respectively, 0.5 R^2 for ρ and 0.4 R^2 for τ_p. The orange power law is the empirical power law for τ_p from Bažant et al. (2003) reported to Mohr-Coulomb criterion with an initial cohesion of 300 Pa (Gaume et al., 2014). The second fit of the power law for ρ compared to D, with an initial density of 100 kg m^{-3} (McClung, 2009b). Two surveys in Mount Albert were added to this plot, EP20DF and EP19FC, to obtain more values but these surveys were not presented because the sampling density and extent were not adequate for spatial modeling.~~

5 Conclusion

The spatial variability of mechanical properties has been measured, compared, and estimated in this study. First, we show that in our dataset, the slab properties exhibit spatial patterns that were different from the weak layer spatial patterns. In fact, the slab properties, both the slab thickness and density, had smaller correlation lengths in their variogram than the weak layer strength. The slab properties had higher fractal dimensions than the weak layer strength, which demonstrates a more "rough" spatial surface. Secondly, we estimated the spatial variability of snow mechanical properties and also some stability metrics using spatial variables of microtopography. Estimates were reliable and precise for snow mechanical properties, but not for stability metrics. We also show the utility of using microtopography to estimate snow spatial variability. However, no microtopographic indicators were predominantly used to give advice to backcountry recreationists. The use of microtopography seems to be specific to each site and snow properties. The use of multiscale microtopographic indicators, such as the topographic position index TPI and the vector ruggedness measure VRM, should be explored in future work to estimate spatial patterns of snow mechanical properties as input for snow mechanical models. This could lead to the development of predictive methods in operational avalanche forecasting services to estimate the avalanche release size using snow cover modeling and mechanical models. Additional work is needed on stability occurrence with respect to microtopography indicators to help backcountry recreationists find a safer downhill and uphill route.

Code and data availability. The code and the data are available upon request.

Author contributions. FM conceptualized and led the research, wrote the code for the processing and analysis of the data, and drafted the manuscript. FG and AL conceptualized the research and reviewed the manuscript. AL provided the major part of the funds for the project.

570 *Competing interests.* Alexandre Langlois is a member of the editorial board of The Cryosphere

Acknowledgements. This project was funded by the Search and Rescue New Initiatives Fund from Public Safety Canada (SAR-NIF), the Natural Sciences and Engineering Research Council of Canada (NSERC)~~and~~, the Quebec Research Funds - Nature and Technologies (FRQNT), and the Canada Foundation for Innovation (CFI) for funding the Station d'études montagnardes des Chic-Chocs (SEM). The authors would like to thank Jeff Goodrich and the Mount Revelstoke and Glacier National Parks staff for their support. This research was
575 also possible with the help of Claude Isabel and the Gaspésie National Park (SEPAQ), and also with the help of Dominic Boucher and Avalanche Québec staff. The authors would also like to thank Jean-Benoît Madore, Julien Meloche, Antoine Rolland, Alex Blanchette, Jacob Laliberté and William Durand for their help on the field. Lastly, we want to thank the two anonymous reviewers for their helpful and constructive comments, which significantly improve the quality of our manuscript.

Appendix A

580 The log-log variograms needed to calculate the fractal dimension are presented in the Appendix.
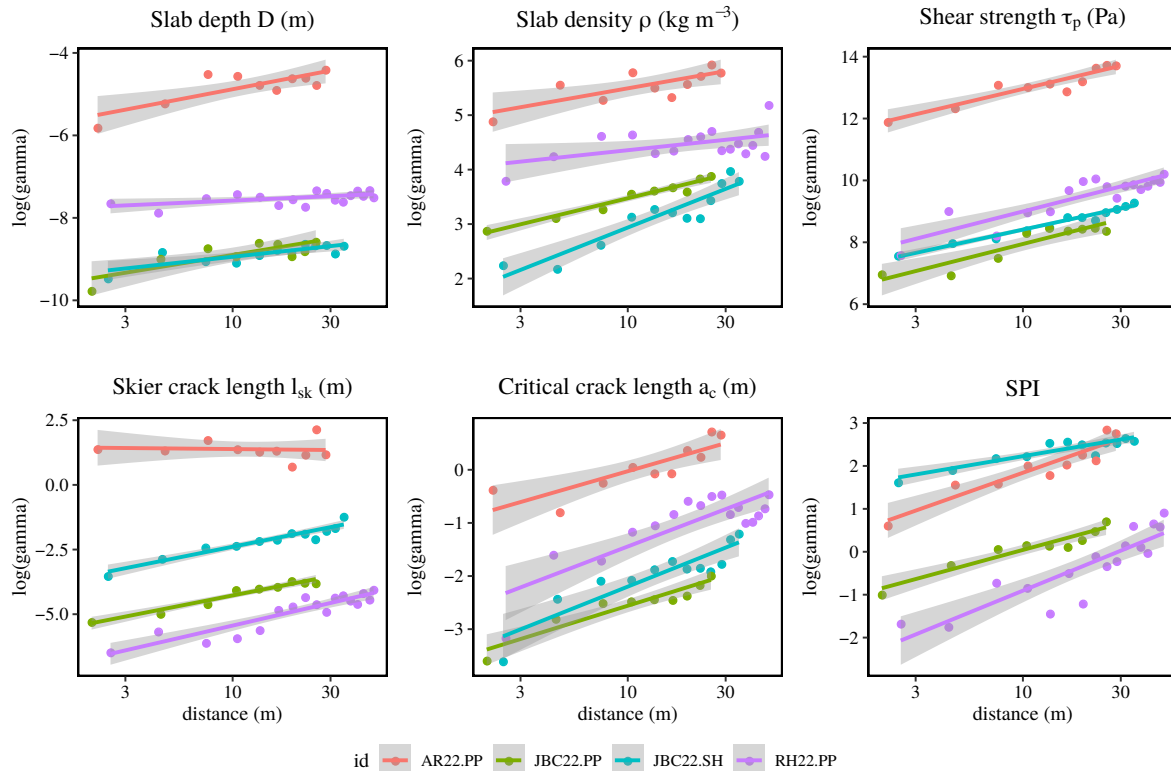
Figure A1. Log-Log variogram of snow mechanical properties and stability metrics for every snow spatial surveys. The fractal dimension is computed from the slope of the regression line. The gamma represented the variance for each variable. The unit is specified in each title.

References

Bažant, Z. P., Zi, G., and McClung, D.: Size effect law and fracture mechanics of the triggering of dry snow slab avalanches, Journal of Geophysical Research: Solid Earth, 108, https://doi.org/10.1029/2002jb001884, 2003.

Bellaire, S. and Schweizer, J.: Measuring spatial variations of weak layer and slab properties with regard to snow slope stability, Cold Regions Science and Technology, 65, 234–241, https://doi.org/10.1016/J.COLDREGIONS.2010.08.013, 2011.

Birkeland, K. W.: Spatial patterns of snow stability throughout a small mountain range, Journal of Glaciology, 47, 176–186, https://doi.org/10.3189/172756501781832250, 2001.

Blöschl, G. and Sivapalan, M.: Scale issues in hydrological modelling: A review, Hydrological Processes, 9, 251–290, https://doi.org/10.1002/hyp.3360090305, 1995.

Calonne, N., Richter, B., Löwe, H., Cetti, C., Judith, Herwijnen, A. V., Fierz, C., Jaggi, M., and Schneebeli, M.: The RHOSSA campaign: Monitoring the seasonal evolution of an alpine snowpack up to daily resolution, in Prep., pp. 1–30, 2019.

Campbell, C. and Jamieson, B.: Spatial variability of slab stability and fracture characteristics within avalanche start zones, Cold Regions Science and Technology, 47, 134–147, https://doi.org/10.1016/j.coldregions.2006.08.015, 2007.

585

590

Canadian Avalanche Association: Observations guidelines and recording standards for weather, snowpack and avalanches, Tech. rep., Revelstoke, 2016.

Chilès, J.-P. and Delfiner, P.: Geostatistics: Modelling Spatial Uncertainty, John Wiley & Sons, Ltd, New-York, 1999.

Conrad, O., Bechtel, B., Bock, M., Dietrich, H., Fischer, E., Gerlitz, L., Wehberg, J., Wichmann, V., and Böhner, J.: System for Automated Geoscientific Analyses (SAGA) v. 2.1.4, Geoscientific Model Development, 8, 1991–2007, https://doi.org/10.5194/GMD-8-1991-2015, 2015.

Dale, M. R. T. and Fortin, M.-J.: Spatial Analysis : A guide for Ecologists, Cambridge University Press, 2nd edn., 2014.

Deems, J. S., Fassnacht, S. R., and Elder, K. J.: Fractal distribution of snow depth from lidar data, Journal of Hydrometeorology, 7, 285–297, https://doi.org/10.1175/JHM487.1, 2006.

Feick, S., Kronholm, K., and Schweizer, J.: Field observations on spatial variability of surface hoar at the basin scale, Journal of Geophysical Research: Earth Surface, 112, 1–16, https://doi.org/10.1029/2006JF000587, 2007.

Föhn, P.: The stability index and various triggering mechanisms, IAHS, 162, 195–214, 1987.

Fyffe, B. and Zaiser, M.: The effects of snow variability on slab avalanche release, Cold Regions Science and Technology, 40, 229–242, https://doi.org/10.1016/j.coldregions.2004.08.004, 2004.

Gao, J. and Xia, Z. G.: Fractals in physical geography, Progress in Physical Geography, 20, 178–191, https://doi.org/10.1177/030913339602000204, 1996.

Gaume, J. and Reuter, B.: Assessing snow instability in skier-triggered snow slab avalanches by combining failure initiation and crack propagation, Cold Regions Science and Technology, 144, 6–15, https://doi.org/10.1016/j.coldregions.2017.05.011, 2017.

Gaume, J., Chambon, G., Eckert, N., and Naaim, M.: Influence of weak-layer heterogeneity on snow slab avalanche release: Application to the evaluation of avalanche release depths, Journal of Glaciology, 59, 423–437, https://doi.org/10.3189/2013JoG12J161, 2013.

Gaume, J., Schweizer, J., Herwijnen, A., Chambon, G., Reuter, B., Eckert, N., and Naaim, M.: Evaluation of slope stability with respect to snowpack spatial variability, Journal of Geophysical Research: Earth Surface, 119, 1783–1799, https://doi.org/10.1002/2014jf003193, 2014.

Gaume, J., Chambon, G., Eckert, N., Naaim, M., and Schweizer, J.: Influence of weak layer heterogeneity and slab properties on slab tensile failure propensity and avalanche release area, Cryosphere, 9, 795–804, https://doi.org/10.5194/tc-9-795-2015, 2015.

Gaume, J., Van Herwijnen, A., Chambon, G., Wever, N., and Schweizer, J.: Snow fracture in relation to slab avalanche release: Critical state for the onset of crack propagation, Cryosphere, 11, 217–228, https://doi.org/10.5194/tc-11-217-2017, 2017.

Gauthier, D. and Jamieson, B.: Evaluation of a prototype field test for fracture and failure propagation propensity in weak snowpack layers, Cold Regions Science and Technology, 51, 87–97, https://doi.org/10.1016/J.COLDREGIONS.2007.04.005, 2008.

Grünewald, T., Schirmer, M., Mott, R., and Lehning, M.: Spatial and temporal variability of snow depth and ablation rates in a small mountain catchment, Cryosphere, 4, 215–225, https://doi.org/10.5194/tc-4-215-2010, 2010.

Guy, Z. M. and Birkeland, K. W.: Relating complex terrain to potential avalanche trigger locations, Cold Regions Science and Technology, 86, 1–13, https://doi.org/10.1016/j.coldregions.2012.10.008, 2013.

Habermann, M., Schweizer, J., and Jamieson, J. B.: Influence of snowpack layering on human-triggered snow slab avalanche release, Cold Regions Science and Technology, 54, 176–182, https://doi.org/10.1016/j.coldregions.2008.05.003, 2008.

Hägeli, P. and McClung, D. M.: Avalanche characteristics of a transitional snow climate-Columbia Mountains, British Columbia, Canada, Cold Regions Science and Technology, 37, 255–276, https://doi.org/10.1016/S0165-232X(03)00069-7, 2003.

Hägeli, P. and McClung, D. M.: Hierarchy theory as a conceptual framework for scale issues in avalanche forecast modeling, Annals of Glaciology, 38, 209–214, https://doi.org/10.3189/172756404781815266, 2004.

Harper, J. T. and Bradford, J. H.: Snow stratigraphy over a uniform depositional surface: Spatial variability and measurement tools, Cold Regions Science and Technology, 37, 289–298, https://doi.org/10.1016/S0165-232X(03)00071-5, 2003.

635 Hesterberg, T., Choi, N. H., Meier, L., and Fraley, C.: Least angle and l1 penalized regression: A review, https://doi.org/10.1214/08-SS035, 2, 61–93, https://doi.org/10.1214/08-SS035, 2008.

Johnson, J. B. and Schneebeli, M.: Characterizing the microstructural and micromechanical properties of snow, Cold Regions Science and Technology, 30, 91–100, https://doi.org/10.1016/S0165-232X(99)00013-0, 1999.

Kronholm, K. and Birkeland, K. W.: Integrating spatial patterns into a snow avalanche cellular automata model, Geophysical Research
640 Letters, 32, https://doi.org/10.1029/2005GL024373, 2005.

Kronholm, K. and Birkeland, K. W.: Reliability of sampling designs for spatial snow surveys, Computers and Geosciences, 33, 1097–1110, https://doi.org/10.1016/j.cageo.2006.10.004, 2007.

Kronholm, K. and Schweizer, J.: Snow stability variation on small slopes, Cold Regions Science and Technology, 37, 453–465, https://doi.org/10.1016/S0165-232X(03)00084-3, 2003.

645 Landry, C., Birkeland, K., Hansen, K., Borkowski, J., Brown, R., and Aspinall, R.: Variations in snow strength and stability on uniform slopes, Cold Regions Science and Technology, 39, 205–218, https://doi.org/10.1016/j.coldregions.2003.12.003, 2004.

Löwe, H. and van Herwijnen, A.: A Poisson shot noise model for micro-penetration of snow, Cold Regions Science and Technology, 70, 62–70, https://doi.org/10.1016/j.coldregions.2011.09.001, 2012.

Lutz, E. and Birkeland, K. W.: Spatial patterns of surface hoar properties and incoming radiation on an inclined forest opening, Journal of
650 Glaciology, 57, 355–366, https://doi.org/10.3189/002214311796405843, 2011.

Lutz, E., Birkeland, K. W., Kronholm, K., Hansen, K., and Aspinall, R.: Surface hoar characteristics derived from a snow micropenetrometer using moving window statistical operations, Cold Regions Science and Technology, 47, 118–133, https://doi.org/10.1016/j.coldregions.2006.08.021, 2007.

Marra, G. and Wood, S. N.: Practical variable selection for generalized additive models, Computational Statistics and Data Analysis, 55,
655 2372–2387, https://doi.org/10.1016/j.csda.2011.02.004, 2011.

McClung, D. M.: Dimensions of dry snow slab avalanches from field measurements, Journal of Geophysical Research: Earth Surface, 114, https://doi.org/10.1029/2007JF000941, 2009a.

McClung, D. M.: Dry snow slab quasi-brittle fracture initiation and verification from field tests, Journal of Geophysical Research: Earth Surface, 114, https://doi.org/10.1029/2007JF000913, 2009b.

660 Meloche, F., Gauthier, F., Langlois, A., and Boucher, D.: The Northeastern Rainy Continental snow climate: A snow climate classification for the Gaspé Peninsula, Québec, Canada, in: International Snow Science Workshop, Innsbruck, Austria, pp. 1025–1029, 2018.

Meloche, J., Langlois, A., Rutter, N., McLennan, D., Royer, A., Billecocq, P., and Ponomarenko, S.: High-resolution snow depth prediction using Random Forest algorithm with topographic parameters: A case study in the Greiner watershed, Nunavut, Hydrological Processes, 36, e14 546, https://doi.org/10.1002/HYP.14546, 2022.

665 Monti, F., Gaume, J., Van Herwijnen, A., and Schweizer, J.: Snow instability evaluation: Calculating the skier-induced stress in a multi-layered snowpack, Natural Hazards and Earth System Sciences, 16, 775–788, https://doi.org/10.5194/nhess-16-775-2016, 2016.

Mott, R., Schirmer, M., and Lehning, M.: Scaling properties of wind and snow depth distribution in an Alpine catchment, Journal of Geophysical Research Atmospheres, 116, 1–8, https://doi.org/10.1029/2010JD014886, 2011.

Mullen, R. S. and Birkeland, K. W.: Mixed Effect and Spatial Correlation Models for Analyzing a Regional Spatial dataset, International snow science workshop, p. 8, 2008.

Nussbaum, M., Walthert, L., Fraefel, M., Greiner, L., and Papritz, A.: Mapping of soil properties at high resolution in Switzerland using boosted geoadditive models, SOIL, 3, 191–210, https://doi.org/10.5194/SOIL-3-191-2017, 2017.

Pielmeier, C. and Marshall, H. P.: Rutschblock-scale snowpack stability derived from multiple quality-controlled SnowMicroPen measurements, Cold Regions Science and Technology, 59, 178–184, https://doi.org/10.1016/j.coldregions.2009.06.005, 2009.

Proksch, M., Löwe, H., and Schneebeli, M.: Density, specific surface area, and correlation length of snow measured by high-resolution penetrometry, Journal of Geophysical Research: Earth Surface, 120, 346–362, https://doi.org/10.1002/2014JF003266, 2015.

Pulwicki, A., Flowers, G. E., Radic, V., and Bingham, D.: Estimating winter balance and its uncertainty from direct measurements of snow depth and density on alpine glaciers, Journal of Glaciology, 64, 781–795, https://doi.org/10.1017/JOG.2018.68, 2018.

R Core: R : A language and environment for statistical computing, 2013.

Reuter, B. and Schweizer, J.: Describing Snow Instability by Failure Initiation, Crack Propagation, and Slab Tensile Support, Geophysical Research Letters, 45, 7019–7027, https://doi.org/10.1029/2018GL078069, 2018.

Reuter, B., Herwijnen, A. V., and Schweizer, J.: Simple drivers of snow instability, Cold Regions Science and Technology, 120, 168–178, http://dx.doi.org/10.1016/j.coldregions.2015.06.016, 2015a.

Reuter, B., Schweizer, J., and Van Herwijnen, A.: A process-based approach to estimate point snow instability, Cryosphere, 9, 837–847, https://doi.org/10.5194/tc-9-837-2015, 2015b.

Reuter, B., Richter, B., and Schweizer, J.: Snow instability patterns at the scale of a small basin, Journal of Geophysical Research: Earth Surface, 121, 257–282, https://doi.org/10.1002/2015JF003700, 2016.

Reuter, B., Proksch, M., Löwe, H., Van Herwijnen, A., and Schweizer, J.: Comparing measurements of snow mechanical properties relevant for slab avalanche release, Journal of Glaciology, 65, 55–67, https://doi.org/10.1017/jog.2018.93, 2019.

Revuelto, J., Billecocq, P., Tuzet, F., Cluzet, B., Lamare, M., Larue, F., and Dumont, M.: Random forests as a tool to understand the snow depth distribution and its evolution in mountain areas, Hydrological Processes, pp. 1–18, https://doi.org/10.1002/hyp.13951, 2020.

Richter, B., Schweizer, J., Rotach, M., and van Herwijnen, A.: Validating modeled critical crack length for crack propagation in the snow cover model SNOWPACK, The Cryosphere Discussions, pp. 1–21, https://doi.org/10.5194/tc-2019-97, 2019.

Rosendahl, P. L. and Weißgraeber, P.: Modeling snow slab avalanches caused by weak-layer failure - Part 2: Coupled mixed-mode criterion for skier-triggered anticracks, Cryosphere, 14, 131–145, https://doi.org/10.5194/tc-14-131-2020, 2020.

Sappington J. Mark, Longshore, K. M., and Thompson, D. B.: Quantifying Landscape Ruggedness for Animal Habitat Analysis: A Case Study Using Bighorn Sheep in the Mojave Desert, The Journal of Wildlife Management, 71, 1419–1426, https://doi.org/10.2193/2005-723, 2007.

Schirmer, M. and Lehning, M.: Persistence in intra-annual snow depth distribution: 2.Fractal analysis of snow depth development, Water Resources Research, 47, 1–14, https://doi.org/10.1029/2010WR009429, 2011.

Schirmer, M., Wirz, V., Clifton, A., and Lehning, M.: Persistence in intra-annual snow depth distribution: 1.Measurements and topographic control, Water Resources Research, 47, 1–16, https://doi.org/10.1029/2010WR009426, 2011.

Schweizer, J. and Kronholm, K.: Snow cover spatial variability at multiple scales: Characteristics of a layer of buried surface hoar, Cold Regions Science and Technology, 47, 207–223, https://doi.org/10.1016/j.coldregions.2006.09.002, 2007.

Schweizer, J. and Reuter, B.: A new index combining weak layer and slab properties for snow instability prediction, Natural Hazards and Earth System Sciences, 15, 109–118, https://doi.org/10.5194/nhess-15-109-2015, 2015.

Schweizer, J., Kronholm, K., Jamieson, J. B., and Birkeland, K. W.: Review of spatial variability of snowpack properties and its importance for avalanche formation, Cold Regions Science and Technology, 51, 253–272, https://doi.org/10.1016/j.coldregions.2007.04.009, 2008a.

Schweizer, J., McCammon, I., and Jamieson, J. B.: Snowpack observations and fracture concepts for skier-triggering of dry-snow slab avalanches, Cold Regions Science and Technology, 51, 112–121, https://doi.org/10.1016/J.COLDREGIONS.2007.04.019, 2008b.

Skøien, J. O. and Blöschl, G.: Sampling scale effects in random fields and implications for environmental monitoring, Environmental Monitoring and Assessment, 114, 521–552, https://doi.org/10.1007/s10661-006-4939-z, 2006.

Stethem, C., Jamieson, B., Schaerer, P., Liverman, D., Germain, D., and Walker, S.: Snow avalanche hazard in Canada - A review, Natural Hazards, 28, 487–515, https://doi.org/10.1023/A:1022998512227, 2003.

Techel, F., Jarry, F., Kronthaler, G., Mitterer, S., Nairz, P., Pavšek, M., Valt, M., and Darms, G.: Avalanche fatalities in the European Alps: Long-term trends and statistics, Geographica Helvetica, 71, 147–159, https://doi.org/10.5194/gh-71-147-2016, 2016.

Trujillo, E., Ramírez, J. A., and Elder, K. J.: Topographic, meteorologic, and canopy controls on the scaling characteristics of the spatial distribution of snow depth fields, Water Resources Research, 43, https://doi.org/10.1029/2006WR005317, 2007.

Veitinger, J., Sovilla, B., and Purves, R. S.: Influence of snow depth distribution on surface roughness in alpine terrain: A multi-scale approach, Cryosphere, 8, 547–569, https://doi.org/10.5194/tc-8-547-2014, 2014.

Veitinger, J., Stuart Purves, R., and Sovilla, B.: Potential slab avalanche release area identification from estimated winter terrain: A multi-scale, fuzzy logic approach, Natural Hazards and Earth System Sciences, 16, 2211–2225, https://doi.org/10.5194/nhess-16-2211-2016, 2016.

Weiss, a.: Topographic position and landforms analysis, Poster presentation, ESRI User Conference, San Diego, CA, 64, 227 – 245, http://scholar.google.com/scholar?hl=en&btnG=Search&q=intitle:Topographic+Position+and+Landforms+Analysis#0, 2001.

Weißgraeber, P. and Rosendahl, P. L.: A closed-form model for layered snow slabs, https://doi.org/10.5194/tc-2022-140.

Westoby, M. J., Brasington, J., Glasser, N. F., Hambrey, M. J., and Reynolds, J. M.: 'Structure-from-Motion' photogrammetry: A low-cost, effective tool for geoscience applications, Geomorphology, 179, 300–314, https://doi.org/10.1016/J.GEOMORPH.2012.08.021, 2012.

Winstral, A., Elder, K., and Davis, R. E.: Spatial snow modeling of wind-redistributed snow using terrain-based parameters, Journal of Hydrometeorology, 3, 524–538, https://doi.org/10.1175/1525-7541(2002)003<0524:SSMOWR>2.0.CO;2, 2002.

Wirz, V., Schirmer, M., Gruber, S., and Lehning, M.: Spatio-temporal measurements and analysis of snow depth in a rock face, Cryosphere, 5, 893–905, https://doi.org/10.5194/tc-5-893-2011, 2011.

Wood, S. N.: Generalized Additive Models, Chapman and Hall/CRC, https://doi.org/10.1201/9781420010404/GENERALIZED-ADDITIVE-MODELS-SIMON-WOOD, 2006.